CAMILO JOSÉ RAMÍREZ LÓPEZ

ASSOCIATION OF SPERM OXIDATIVE STRESS, PROTEOMICS AND FATTY ACID PROFILES IN NELLORE BULLS AT SEXUAL REST

Thesis submitted to the Veterinary Medicine Graduate Program of the Universidade Federal de Viçosa in partial fulfillment of the requirements for the degree of *Doctor Scientiae*.

Adviser: Simone Eliza Facioni Guimarães

VIÇOSA – MINAS GERAIS
2023

Ficha catalográfica elaborada pela Biblioteca Central da Universidade Federal de Viçosa - Campus Viçosa

T
R173a
2023

Ramírez López, Camilo José, 1990-
Association of sperm oxidative stress, proteomics and fatty acid profiles in nellore bulls at sexual rest / Camilo José Ramírez López. – Viçosa, MG, 2023.
1 dissertação eletrônica (84 f.): il. (algumas color.).

Texto em inglês.
Orientador: Simone Eliza Facioni Guimarães.
Tese (doutorado) - Universidade Federal de Viçosa, Departamento de Veterinária, 2023.
Inclui bibliografia.
DOI: https://doi.org/10.47328/ufvbbt.2023.184
Modo de acesso: World Wide Web.

1. Nelore (Bovino) - Reprodução. 2. Sêmen. 3. Antioxidantes. 4. Proteínas. 5. Lipídios. I. Guimarães, Simone Eliza Facioni, 1966-. II. Universidade Federal de Viçosa. Departamento de Veterinária. Programa de Pós-Graduação em Medicina Veterinária. III. Título.

CDD 22. ed. 636.2082

Bibliotecário(a) responsável: Alice Regina Pinto Pires CRB-6/2523

CAMILO JOSÉ RAMÍREZ LÓPEZ

ASSOCIATION OF SPERM OXIDATIVE STRESS, PROTEOMICS AND FATTY ACID PROFILES IN NELLORE BULLS AT SEXUAL REST

Thesis submitted to the Veterinary Medicine Graduate Program of the Universidade Federal de Viçosa in partial fulfillment of the requirements for the degree of *Doctor Scientiae*.

APPROVED: March 31, 2023

Assent:

Camilo José Ramírez López
Autor

Simone Eliza Facioni Guimarães
Adviser

DEDICATION

To God, to my family, to my masters,
to friends, and to all the people who
contributed to making this
a achievement a reality

ACKNOWLEDGMENT

To God, for guiding my steps along the right path and for putting great people on my path.

To my life partner Lidiany for all the support, patience, and unconditional love.

To my beloved son Emilio, for being my greatest motivation and source of inspiration.

To my mother and sisters, for the love and support they never denied me, even in the most difficult situations.

To my adviser Simone Eliza Facioni Guimarães, for the opportunity, confidence, and, above all, friendship.

To my friend and Jose Domingos Guimarães for all the teachings and experiences lived during all this time.

To Professor Maria Cristina Baracat, for welcoming me and opening the doors of her laboratory, and for all her guidance throughout this process.

To my friends Edvaldo Barros and Pedro Vidigal for their dedication and willingness to make our work even better.

To Agropecuária CFM LTDA, for making the animals available for this study.

To the Núcleo de Análise de Biomoléculas for the availability of facilities to carry out this work.

To Juliana Rodrigues, Victor Petro, Victor Gomez, Hernando Ospino, and Karina Vasquez my great friends, thank you for the good times and great memories.

To the Coordenação de Aperfeiçoamento de Pessoal de Nível Superior (CAPES), to granting the scholarship.

This study was financed in part by the Coordenação de Aperfeiçoamento de Pessoal de Nível Superior – Brasil (CAPES) – Finance Code 001.

To coordinate the Veterinary Medicine Graduate Program for funding the analyzes by LC-MS/MS.

To Rosineia Cunha, secretary of the Veterinary Medicine Graduate Program for being our guardian angel here at UFV.

To the Universidade Federal de Viçosa and the Department of Veterinary Medicine, for the opportunity to continue growing on a personal and professional level.

For all the love, patience, willingness, and support thank you all so much.

ABSTRACT

LÓPEZ, Camilo José Ramírez**,** D.Sc., Universidade Federal de Viçosa, March, 2023. **Association of sperm oxidative stress, proteomics and fatty acid profiles in nellore bulls at sexual rest.** Adviser: Simone Eliza Facioni Guimarães.

This study was carried out with the objective of determining the effect of sexual rest on the oxidative status of spermatozoa from adult Nellore bulls and its effect on the fatty acid composition and protein profile. Six bulls were used, which were submitted to Breeding Soundness Evaluation and consecutive semen collection by the electroejaculation method. For each semen collection, the physical and morphological characteristics of the ejaculates were evaluated using conventional optical microscopy and phase contrast microscopy. After analyzing the semen qualitative parameters, the first and last ejaculate of each were centrifuged to separate the spermatozoa from the seminal plasma. From sperm aliquots, the enzymatic activity of Super Oxido Dismutase, Catalase and Glutathione S-Transferase was determined by colorimetric methods. The markers of lipid peroxidation, malondialdehyde and nitric oxide were also determined. Using gas chromatography, the fatty acids of sperm from the first and last ejaculate were identified. For proteomic analysis, total sperm proteins were extracted and precipitated in a 4% CHAPS solution, then quantified by the Bradford method and subsequently analyzed by monodimensional short-run electrophoresis and mass spectrometry (LC-MS/MS). Proteins were identified using PEAKS software version 7.0. Proteins were functionally classified by the RPSBLAST tool of BLAST version 2.13.0 into categories from the KOG database. For the label-free quantitative proteomics analysis, proteins identified in at least three technical replicates of each group with a fold-change greater than 1.5 times were included. Data were analyzed using GraphPad Prism software version 9.1. Four semen collections were necessary so that the bulls at sexual rest presented sperm parameters compatible with reproductive fitness. Differences ($p<0.05$) were observed between all physical and morphological characteristics of the first and last ejaculate. A total of 974 proteins were identified, of which 735 were common between the two groups and 123 and 116 proteins were unique to spermatozoa from the first and last ejaculate, respectively. Functional classification analysis revealed that KOG categories with the highest number of classified proteins were Posttranslational modification, protein turnover, chaperones and Cytoskeleton and Signal transduction mechanisms. The protein abundance profile showed that 6 proteins were differentially abundant in spermatozoa from the first ejaculate and 30 proteins were

differentially abundant in spermatozoa from the last ejaculate. In addition, gas chromatography analysis allowed the identification of 19 fatty acids, 47.3% of the saturated type and 52.7% of the unsaturated type. The C12:0 and C18:0 fatty acids showed difference between the two groups, being more abundant in the spermatozoa of the last ejaculate. The results indicate that oxidative stress may be related to sperm characteristics displayed by bulls at sexual rest, since the accumulation of by-products of lipid peroxidation can cause alterations in the metabolic pathways used by spermatozoa to generate energy used for motility and alter fluidity. of the membrane causing sperm abnormalities.

Keywords: Bovine. Semen. Antioxidants. Lipids. Proteins.

RESUMO

LÓPEZ, Camilo José Ramírez**,** D.Sc., Universidade Federal de Viçosa, março de 2023. **Associação de estresse oxidativo espermático, proteômica e perfis de ácidos graxos em touros nelores em repouso sexual.** Orientadora: Simone Eliza Facioni Guimarães.

Este estudo foi realizado com o objetivo de determinar o efeito do repouso sexual sobre o estado oxidativo de espermatozóides de touros Nelore adultos e seu efeito sobre a composição de ácidos graxos e perfil protéico. Foram utilizados seis touros, os quais foram submetidos à avaliação andrológica e consecutivas coletas de sêmen pelo método de eletroejaculação. Para cada coleta de sêmen, as características físicas e morfológicas dos ejaculados foram avaliadas por meio de microscopia óptica convencional e microscopia de contraste de fase. Após análise dos parâmetros qualitativos do sêmen, o primeiro e o último ejaculado de cada um foram centrifugados para separar os espermatozóides do plasma seminal. A partir de alíquotas de esperma, a atividade enzimática de Super Oxido Dismutase, Catalase e Glutationa S-Transferase foi determinada por métodos colorimétricos. Os marcadores de peroxidação lipídica, malondialdeído e óxido nítrico também foram determinados. Usando cromatografia gasosa, foram identificados os ácidos graxos do esperma do primeiro e do último ejaculado. Para análise proteômica, as proteínas totais do esperma foram extraídas e precipitadas em solução CHAPS a 4%, quantificadas pelo método de Bradford e posteriormente analisadas por eletroforese monodimensional de curta duração e espectrometria de massas (LC-MS/MS). As proteínas foram identificadas usando o software PEAKS versão 7.0. As proteínas foram classificadas funcionalmente pela ferramenta RPSBLAST do BLAST versão 2.13.0 em categorias do banco de dados KOG. Para a análise proteômica quantitativa label-free, foram incluídas as proteínas identificadas em pelo menos três réplicas técnicas de cada grupo com um fold-change superior a 1,5 vezes. Os dados foram analisados usando o software GraphPad Prisma versão 9.1. Foram necessárias quatro coletas de sêmen para que os touros em repouso sexual apresentassem parâmetros espermáticos compatíveis com a aptidão reprodutiva. Diferenças ($p<0,05$) foram observadas entre todas as características físicas e morfológicas do primeiro e último ejaculado. Um total de 974 proteínas foram identificadas, das quais 735 eram comuns entre os dois grupos e 123 e 116 proteínas eram exclusivas dos espermatozóides do primeiro e do último ejaculado, respectivamente. A análise da classificação funcional revelou que as categorias KOG com maior número de proteínas classificadas foram Modificação pós-

traducional, renovação de proteínas, chaperonas e Mecanismos de transdução de citoesqueleto e sinal. O perfil de abundância de proteínas mostrou que 6 proteínas foram diferencialmente abundantes nos espermatozóides do primeiro ejaculado e 30 proteínas foram diferencialmente abundantes nos espermatozóides do último ejaculado. Além disso, a análise por cromatografia gasosa permitiu a identificação de 19 ácidos graxos, sendo 47,3% do tipo saturado e 52,7% do tipo insaturado. Os ácidos graxos C12:0 e C18:0 apresentaram diferença entre os dois grupos, sendo mais abundantes nos espermatozoides do último ejaculado. Os resultados indicam que o estresse oxidativo pode estar relacionado às características espermáticas apresentadas pelos touros em repouso sexual, uma vez que o acúmulo de subprodutos da peroxidação lipídica pode causar alterações nas vias metabólicas utilizadas pelos espermatozóides para gerar energia utilizada para a motilidade e alterar a fluidez da membrana causando anormalidades espermáticas.

Palavras-chave: Bovinos. Sêmen. Antioxidantes. Lipídios. Proteínas.

LIST OF ILLUSTRATIONS

Figure 1. Seminal characteristics of Nellore bulls at rest and during sexual activity. Medians and interquartile ranges of ejaculates and sperm quality parameters. MOT: Sperm Motility; VIG: Sperm Vigor; DefT: Sperm Total Defects; Con: Sperm Concentration; Asp: Ejaculate Aspect; MM: Sperm Mass Motility; Vol: Ejaculate Volume. *p<0,05; **p<0,01; ***p<0,001. 45

Figure 2. Antioxidant enzyme activity and oxidative/nitrosative stress markers in sperm extract from Nellore bulls at rest and during sexual activity. The column represents the mean value; whiskers represent the maximum data. Superoxide Dismutase; CAT: Catalase; GST: Glutathione-S-Transferase; MDA: Malondialdehyde; NO: Nitric Oxide. *p<0,05; **p<0,01. 46

.

Figure 3. Relative abundance of Fatty Acids identified in sperm extract from Nellore bulls at rest and during sexual activity. A: relative quantification of total FA identified; B: relative quantification of FA excluding the most abundant. The column represents the mean value; whiskers represent the standard deviation. ***Significant difference (p<0.001) between ejaculates. 47

Figure 4. Proteomics profile of sperm extract from Nellore bulls at rest and during sexual activity. From the total of 974 proteins, 858 were identified in the spermatozoa of the first ejaculate (Group A) and 851 in the spermatozoa of the fourth ejaculate (Group B). The intersection shows 735 proteins conserved in both spermatozoa groups. Group A has 123 unique proteins while Group B has 116 unique proteins. 48

Figure 5. Functional classification of sperm extract proteins from Nellore bulls at rest and during sexual activity. The sequence similarity searches classified 749 proteins into four main groups of the KOG database. One hundred proteins did not show significant hits [NH] and were not classified. The twenty-six letters from [A] to [Z] represent the functional categories of the KOG database. “Posttranslational modification, protein turnover, chaperones” [O] and “Energy production and conversion” [C] were the categories with the highest number of annotated proteins. 49

Figure 6. differentially abundant proteins in sperm extract from Nellore bulls at rest and during sexual activity. The label-free quantification analysis identified 36 differentially abundant proteins (DAP) in the spermatozoa of bulls in sexual rest. The heatmap shows the distribution of DAP abundance values in technical replicates. The colors represent the peak area values submitted to the row scale. Red squares indicate high abundance, and green squares indicate low one. Group A: spermatozoa first ejaculate; Group B: spermatozoa of fourth ejaculate.

LIST OF TABLES

Table S1. Semen phenotypic parameters of Nellore bulls in sexual rest. Physical and morphological parameters of the semen of Nellore bulls collected by the electroejaculation method and evaluated by microscopy. 51

Table S2. Profile of Fatty acid in in sperm extract from Nellore bulls at rest and during sexual activity. Numeric abbreviation, trivial name, and a class of FA identified by GCFID. 52

Table S3. Total protein identified in in sperm extract from Nellore bulls at rest and during sexual activity. The proteins were identified using Peaks v.7 software. 52

Table S4. Differentially abundant proteins in sperm extract from Nellore bulls at rest and during sexual activity. The abundance of the proteins was estimated by peak area. 75

LIST OF ACRONYMS AND ABBREVIATIONS

ACN	Acetonitrile
ATP	Adenosine Triphosphate
CAT	Catalase
CHAPS	3-3-cholamidopropyl dimethylammonium-1-propane sulfonate
DTT	Dithiothreitol
DEP	Differentially Expressed Proteins
FA	Fatty Acids
FDR	False Discovery Rate
FID	Flame Ionization Detector
GC	Gas Chromatography
GST	Glutathione S-Transferase
LC	Liquid Chromatography
LPO	Lipid Peroxidation
MDA	Malonaldehyde
MS	Mass spectrometer
PSS	Postmeiotic Sperm Senescence
PUFA	Polyunsaturated Fatty Acids
ROS	Reactive Oxygen Species
NO	Nitric Oxide
SDS-PAGE	Sodium Dodecyl Sulfate-PolyAcrylamide Gel Electrophoresis
SMC	Smooth Muscle Cells
SOD	Superoxide Dismutase
SR	Sexual rest

SUMMARY

1. INTRODUCTION 14

2. OBJECTIVES 16

3. LITERATURE REVIEW 17

4. REFERENCES 22

5. Oxidative stress associated with proteomic and fatty acid profiles of sperm from Nellore bulls at rest. 26

5.1. Introduction 28

5.2. Results 29

5.3. Discussion 32

5.4. Conclusions 38

5.5. Methods 38

5.6. Fgures 45

5.7. Tables 51

5.8. References 76

6. FINAL CONSIDERATIONS 84

1. INTRODUÇÃO

Beef cattle raising in Brazil represents one of the commercial activities with the greatest impact on federal revenue, responsible for driving the national economy through the generation of millions of direct and indirect jobs and annual revenues of billions of reais resulting from the export of millions of tons of meat to different places in the world.

Despite fluctuations in national and international markets, beef production has shown constant growth in recent years, as a result of decades of investment in agricultural technology, implementation of rigorous genetic improvement programs and the widespread use of reproductive biotechnologies that impact directly on reproductive efficiency. The application of these strategies helped, among other factors, to consolidate Brazil as the second largest producer of beef in the world, responsible for producing 13.6% of the world's beef in 2022 (ABIEC, 2022).

The activity of creating, recreating and fattening cattle is however exposed to a series of variations inherent to its production characteristics that can compromise the productivity of the sector. Particularly, variations in the prices of agricultural inputs and raw materials used in animal feed, added to the costs of implementing sanitary protocols and replacing matrices and breeding bulls, represent serious bottlenecks for the sustainability of the primary meat chain. However, variations in reproductive indices are considered the main influencers of zootechnical indicators of meat production systems, since they are directly related to the production of calves, the main element of the meat industry (Castro et al., 2018).

The reproductive rates of beef cattle in Brazil remain low in relation to their actual production potential. The high age at first calving, a long calving interval and low pregnancy, birth and weaning rates are factors that reduce reproductive efficiency. However, all these factors are linked to inadequate management and incorrect reproductive planning of the herd. In this sense, the choice of matrices and breeding bulls play a transcendental role in the financial health of the rural Company (Moorey and Biase, 2020).

The choice of healthy and fertile sires is fundamental, since when serving a high number of females, the bulls will directly influence the fertility of the herd and, consequently, the production of calves (Ugur et al., 2022). It is estimated that a high percentage of bulls in service are infertile or subfertile.

The causes of fertility disorders are multifactorial and may be linked to genetic factors or testicular degeneration, delayed sexual maturity, testicular hypoplasia, spermiogenesis imperfecta, immaturity or sexual rest (Memili et al., 2012). Sexual rest can compromise pregnancy rates in cattle herds due to its periodic appearance, causing the accumulation of spermatozoa in the tails of the epididymis, leaving them exposed, probably to the effect of reactive oxygen species (ROS) generated by cellular aerobic metabolism (Barth, 2007). The ROS attack on sperm cell macromolecules may be related to the phenotypic characteristics of resting bull ejaculates.

Therefore, our objective was determine the effect of sexual rest on the oxidative state of spermatozoa of adult Nellore bulls and its effect on fatty acid composition and proteomic profile

2. OBJECTIVES

2.1. Main objetive

- To determine the effect of sexual rest on the oxidative status of spermatozoa of adult Nellore bulls and its effect on fatty acid composition and proteomic profile.

2.2. Specific objectives

- To determine the oxidative status of spermatozoa from bulls at sexual rest and its relationship with sperm motility, sperm vigor, sperm total defects, sperm concentration, ejaculate aspect, sperm mass motility, ejaculate volume.

- To determine the fatty acid composition of sperm from adult Nellore bulls in sexual rest condition.

- To determine the proteomic profile of sperm from adult Nellore bulls and the changes in protein caused by sexual rest.

3. LITERATURE REVIEW.

3.1. Role of epididymis in sperm viability:

Mammalian spermatozoa are unable to move or establish successful interactions with the cumulus-oocyte complex after exiting the testes despite being morphologically complete. To become fertile, spermatozoa must first undergo several stages of postgonadal differentiation that occur mostly during their transit along several meters of epididymis (Dickson, 2015).

The epididymis is an unbranched, highly convoluted, specialized tubular organ that connects the efferent ducts and drains the testes into the deferent ducts of the male reproductive system, tasked, among other things, with serving as a channel for transporting sperm to the organs of the female reproductive system. (Dacheux et al., 2009).

Anatomically, the epididymis is divided into four regions (initial segment, head, body and tail) histologically and functionally distinct, lined with an epithelium composed of five types of cells (main, basal, narrow, clear and dendritic cells) responsible for secretion and absorption of specific molecules that make the epididymal luminal environment unique and conducive to functional sperm transformation or sperm maturation (Sullivan et al., 2015).

Although the anatomical division of the epididymis is not strictly considered in all mammalian species, the function of each of them is clearly defined, in this way, the initial segment is responsible for absorbing most of the testicular fluid that enters the epididymis leading to a pronounced concentration of luminal spermatozoa. From that point on, the head of the epididymis is more active in terms of protein synthesis and secretion, initiating a series of sperm modifications such as the migration of the cytoplasmic droplet, the beginning of the flagellar beat and the ability to bind to the zona pellucida (Paul et al., 2021).

These functional characteristics continue to be developed in the body of the epididymis before reaching an adequate level in the caudal segment. This last region is characterized by exhibiting a relatively larger lumen and its surrounding epithelial cells show strong absorptive activity, attributes in line with the main function of the epididymal tail in terms of forming a sperm storage reservoir (James et al., 2020).

In addition to acting as the site where sperm maturation takes place and serving as an extra-gonadal reservoir for sperm, the epididymis also have the ability to preserve the viability of stored gametes for a limited time. This preservation is mainly linked to the inhibition of sperm motility associated with a reduction in their metabolic rate (Sullivan, 2015).

Some influences external to spermatozoa are involved in the control of their motility, for example, the reduction of scrotal temperature in relation to body temperature, low oxygen content in the epididymal tissue, absence of glucose in the luminal fluid and the ionic variations of the components of the epididymal fluid, such as calcium and bicarbonate concentrations resulting from water reabsorption in the initial segment through aquaporin channels driven by the transepithelial movement of ions such as sodium, chlorine and bicarbonate (Dickson, 2015).

Thus, the inactivation of sperm-specific Ca^{+} and K^{+} channels, involved in sperm capacitation, acidify the pH of the epididymal environment through the pumping of protons and the absorption of bicarbonate by the clear cells of the caudal segment of the epididymis, becoming the main cellular mechanism for maintaining sperm quiescence during their maturation and storage in the epididymis (Nixon et al., 2019).

The mean time required for sperm flow in the epididymis ranges from 8 to 11 days in bulls, with transit in the head and body segment of the epididymis constant (4 days) and not influenced by the frequency of ejaculations, age or environmental conditions, while the transit time through the tail of the epididymis may be accelerated in situations where ejaculatory frequency is increased (Amann et al., 1976).

Despite their intrinsic ability to move, the movement of sperm through the epididymis is mainly attributed to rhythmic contractions of the smooth muscles that surround the epididymal tubule, stimulated by adrenergic innervation and the action of hormones such as prostaglandins and oxytocin (Fernandez et al., 2016).

The smooth muscle cells (SMC) of the epididymal ducts and efferent ducts have morphophysiological changes that accompany the functional characteristics according to the anatomical region. Thus, the SMC of the proximal regions of the epididymis are smaller in number and size in relation to the same cell population in the most distal region of the epididymis tail, in addition to presenting biochemically different amounts and types of adrenergic receptors, which would explain the changes in the pattern of contractility exhibited (Baumgarten et al., 1971).

The muscular layer becomes thicker towards the distal segments and, as a result of peristaltic contractions, the muscular layer of the epididymis controls the passage of increasing concentrations of sperm. Peristalsis induces an increasing hydrostatic pressure gradient towards the tail, resulting in forward and downward transport of sperm contents, leading to a functional

mixing of the luminal contents, in addition to facilitating the transport of these spermatozoa towards the distal end of the epididymis (Rodriguez et al., 2021).

In the cauda epididymis and proximal vas deferens (both components of the functional terminal segment), the smooth muscle layer is not only thicker, but in this section there are two layers of muscles that contract to induce the emission of sperm during ejaculation, these contractions resulting from different neuronal signaling in the head region, do not present spontaneous contractions, among other things due to the physiological need to keep the spermatozoa located in this region in a quiescent state (Elfen et al., 2018).

Despite the absence of spontaneous contractions, the SMC of the distal tail have larger nerve inversion fibers and a greater number of alpha1-adrenergic receptors, responsible for binding noradrenaline, the hormone responsible for triggering stimulation of the SMC of the tail of the epididymis during ejaculation. Noradrenaline is the greatest stimulator of the SMC of the cauda epididymis, however, it is not the only substance to stimulate muscle contraction, concentrations of ions such as magnesium and calcium, and peptides such as Neuropeptide Y and Vasoactive Intestinal Polypeptide (VIP) and other types of neurotransmitters are involved in SMC stimulation, making the contractility process a complex mechanism (Mewe et al., 2008).

Conductivity alterations of the nerve fibers that innervate the SMC of the epididymis have been identified as a possible cause of sperm accumulation during sexual rest, however, it is believed that environmental circumstances and social interaction can also influence the condition of sexual rest (Cattelan and Gasparini, 2021). Absence of females of reproductive age, mating frequency, climatologically unfavorable periods and the presence of other dominant males have been related to the inhibition of sexual behavior and, consequently, to the accumulation of sperm (Firman et al., 2015).

In other species, the accumulation of sperm causes postmeiotic sperm senescence (PSS), a phenomenon that affects haploid male gametes and is characterized by damage to chromatin, mitochondria and membranes, probably due to the accumulation of toxic waste and free radicals produced by spermatozoa establishment of a state of oxidative stress (Pizzari et al., 2007, Hettyey et al., 2012). PSS is an irreversible cellular condition that occurs between spermiogenesis and fertilization and is determined by the individual cell age and, therefore, is independent of male age (Reinhardt, 2007, Vega et al., 2019).

3.2. Role of reactive oxygen species in sperm viability:

The reactive oxygen species (ROS) are short-lived and muscle-sized reactive molecules that belong to the class of free radicals, derived from oxygen and characterized by the presence of one or more unpaired electrons in their outer layer. Due to their unstable chemical structure, they attack nearby organic molecules such as lipids, proteins, and DNA to reach an equilibrium state. The most common ROS include superoxide anion, hydroxyl radicals, peroxyl radicals, alkoxyl radicals, organic hydroperoxides, and hydrogen peroxide. Furthermore, nitrogen-based free radicals, such as peroxynitrites and nitric oxide, also constitute an important subclass of ROS (Baskaran et al., 2020, Wagner et al., 2018).

The most important source of endogenous free radicals is the mitochondria, organelles responsible for the production of cellular energy in the form of ATP. In the inner mitochondrial membrane, different substrates are oxidized and reduced through the electron transport chain complex, generating a flow of electrons that ends with the synthesis of ATP and the reduction of molecular oxygen to water. Although this process is highly efficient, a small percentage of oxygen is reduced to superoxide by simple transfer mediated by Complex I and III (Kopper et al., 2008, Agarwal et al., 2014).

At physiological levels, ROS function as signaling molecules and are crucial for normal cellular functions. However, excessive levels of ROS lead the cellular reductive-oxidative balance to an oxidative state, which impairs the physiological functions of macromolecules, causing cellular damage (Walters et al., 2018). Cells have an antioxidant defense system that regulates pro-oxidant levels and protects cells from the harmful effects of free radicals. These defenses are classified into enzymatic and non-enzymatic antioxidants. Enzymatic antioxidants include superoxide dismutase, catalase, and glutathione peroxidase. While non-enzymatic antioxidants are made up of vitamins, coenzymes Q10, β-carotenes, selenium, and zinc, which act as cofactors for many antioxidant enzymes (Tvrda et al., 2011). Redox proteins are structurally characterized by the presence of catalytic sites that can accept or donate electrons. The ability to mediate electron transfer makes them key proteins in reductive-oxidative reactions that take place in various biological processes.

At low levels, ROS actively participates in the metabolic pathways during sperm activation, which leads to cholesterol efflux, production of cyclic adenosine monophosphate (cAMP) and tyrosine phosphorylation by inhibiting tyrosine phosphatase, stimulating capacitation and hyperactivation sperm formation, acrosomal reaction and chromatin

compaction in maturing spermatozoa, by helping the disulfide bond formed by cysteine residues of protamines, ensuring chromatic stability and preventing chromosomal DNA damage (Plessi et al., 2015, Peña et al., 2021). ROS, especially peroxides, also play a role in the formation of the mitochondrial capsule, which is formed by a network of proteins with several disulfide bonds that prevent the proteolytic degradation of mitochondria (Baskaran et al., 2020, Aiken, 2020).

ROS essentially participates in increasing plasma membrane fluidity during sperm-oocyte fusion, mediating the activation of biochemical cascades for capacitation followed by a successful acrosomal reaction (Bromfield et al., 2015). Throughout the entire duration of sperm capacitation, ROS prevents the deactivation of phospholipase A2 by inhibiting protein tyrosine phosphatase activity. Thus, activated phospholipase A2 potentially cleaves secondary fatty acid from membrane phospholipid triglycerides and increases plasma membrane fluidity (Dutta et al., 2020).

4. REFERÊNCIAS BIBLIOGRÁFICAS

Associação Brasileira das Industrias Exportadoras de Carne. Beef Report: Perfil da pecuária no Brasil. 2022.

Agarwal A, Virk G, Ong C, Plessis S. Effect of oxidative stress on male reproduction. **The Journal of Men´s Health.** 32(1): 1-17, 2014.

Amam R, Johnson L, Thompson D, Pickett B. Daily spermatozoal production, epididymal spermatozoal reserves and transit time of spermatozoa through the epididymis of the rhesus monkey. **Biology of Reproduction.** 15(5): 586-592 1976.

Aitken J. Impact of oxidative stress on male and female germ cells: implications for fertility. **Reproduction.** 159(4): 189-201, 2020.

Barth, A. Sperm accumulation in the ampullae and cauda epididymides of bulls. **Animal Reproduction Science**. 102(3): 238-246, 2007.

Baskaran S, Finelli R, Agarwal A, Henkel R. Reactive oxygen species in male reproduction: A boon or a bane? **Andrologia.** 53(1): 13577, 2020.

Baumgarten H, Holstein A, Rosengren E. Arrangement, ultrastructure, and adrenergic innervation of smooth musculature of the ductile efferents, ductus epididymis and ductus deferens of man. **Z. Zellforsch.** 120, 37–79, 1971.

Bromfield E, Aitken J, Anderson L, McLaughlin A, Nixon B. The impact of oxidative stress on chaperone-mediated human sperm–egg reaction. **Human Reproduction**. 30:2597–2613, 2015.

Castro F, Fernandes H, Leal C. Sistemas de manejo para maximização da eficiência reprodutiva em bovinos de corte nos trópicos. **Veterinaria e Zootecnia.** 25(1): 41-61, 2018.

Cattelan S, Gasparini C. Male sperm storage impairs sperm quality in the zebrafish. **Scientific Report.** 11: 16689, 2021.

Dacheux J, Belleannee C, Jones R, Labas V, Belghazi M, Guyonnet B, Druart X, Gatti J, Dacheux F. Mammalian epididymal proteome. **Molecular and Cellular Endocrinology.** 306, 45-50, 2009.

Dickson V. Odyssey of the spermatozoon. **Asian Journal of Andrology,** 17, 522-528, 2015.

Dutta S, Henkel R, Sengupta P, Agarwal A. Physiological role of ROS in sperm fuction. In: **Male Infertility**. Parekattil S, Esteves S, Agarwal A. (eds). Springer, Cham. 337-345, 2020.

Elfgen V, Mietens A, Mewe M, Hau T, Contractility of the epididymal duct: function, regulation and potential drug effects. **Reproduction,** 156 (4):125-141, 2018

Fernandez B, Narciandi F, O´Farrelly C, Kelly A, Fair S, Meade K, Lonergan P. Cauda Epididymis-Specific Beta-Defensin 126 Promotes Sperm Motility but NotFertilizing Ability in Cattle. **Biology of Reproduction,** 95(5): 1-12, 2016.

Firman R, Young F, Rowe D, Doung H, Gasparini C. Sexual rest and pos-meiotic sperm ageing in house mice. **Journal of Evolutionary Biology.** 28(7): 1373-1382, 2015.

Hettyey A, Vági B, Penn D, Hoi H, Wagner R. Post-Meiotic Intra-Testicular Sperm Senescence in a Wild Vertebrate. **Plos One**. 2012.

James E, Carrel D, Aston K, Jenkins T, Yeste M, Salas A. The role of epididymis aepididymisontribution of epidymosomes to mammalian reproduction. **International Journal of Molecular Sciences,** 21 (15):5377, 2020.

Koppers A, De Iuliis G, Finnie J, McLaughlin E, Aitken J. Significance of mitochondrial reactive oxygen species in the generation of oxidative stress in spermatozoa, ***Journal of Clinical Endocrinology e Metabolism.*** 93(8): 3199–3207, 2008.

Memili E, Dogan S, Rodriguez-Osorio N, Wang X, Oliveira R, Mason M, Govindaraju A, Grant K, Belser L, Crate E, Moura A, Kaya A. Makings of the best spermatozoa: molecular determinants of high fertility. In: Male Infertility. Bashamboo A. (eds). InTech. 2012.

Mewe M, Wulfsen I, Middendorff R, Bauer C. differential modulation of bovine epididymal activity by oxytocin and noradrenaline. **Reproduction,** 134 (3):493-501, 2007.

Moorey S, Biase F. Beef heifer fertility: importance of management practices and technological advancements. **Journal Animal Science and Biotechnology.** 11(1): 97, 2020.

Nixon B, De lullis G, Hart H, Bromfield E, Larsen M, Dun M. Proteomic profiling fo mouse epidymosomes reveals their contributions to post-testicular maturation. **Molecular and Cellular Proteomics,** 18(1):91-108, 2019.

Paul N, Roa t, Nag P, Kumaresn A. Epididymosomes: A potential influencer. **Andrologia,** 53(9): e14155, 2021.

Peña F, Ortiz J, Gaitskell g, Gil M, Ortega C, Martín F. Na integrated overview on the regulation of sperm metabolism (glycolysis-Krebs cycle-oxidative phosphorylation). **Animal Reproduction Science.** In press. 2021.

Pizzari T, Dean R, Pacey A, Moore H, Bonsall M. The evolutionary ecology of pre- and post-meiotic sperm senescence. **Trends in Ecology and Evolution.** 23(3): 131-140, 2007.

Plessis S, Agarwal A, Mohanty G, Van der Linde M. Oxidative phosphorylation versus glycolysis: what fuel do spermatozoa use? **Asian Journal of Andrology.** 17(2): 230-235, 2015.

Reinhardt K. Evolutionary consequences of sperm cell aging. **The Quarterly Review of Biology.** 82(4): 375-393, 2007.

Rodriguez H, Roca J, Rodriguez M, Martinez C. How does the boar epididymis regulate the emission of fertile spermatozoa? **Animal Reproduction Science,** in press, 2021.

Sullivan R. Epididymosomes: a heterogeneous population of microvesicles with multiple functions in sperm maturation and storage. **Asian Journal of Andrology,** (5):726-729, 2015

Tvrdá E, Knazicka Z, bardos L, Massányi P, Lukác N. Impact of oxidative stress on male fertility – a review. **Acta Veterinaria Hungarica.** 59 (4): 465-484, 2011

Vega R, Fox R, Carrasco M, Head M, Jennions M. The effects of male age, sperm age and mating history on ejaculate senescence. **Functional Ecology.** 33(7): 1267.1279, 2019.

Ugur M, Guerreiro D, Moura A, Memili E. Identification of biomarkers of bull fertility using functional genomics. **Animal Reproduction.** 19(1): e20220004, 2022.

Wagner H, Cheng J, Ko E. Role of reactive oxygen species in male infertility: An updated review of literature. **Arab Journal of Urology**. 16 (1): 35-43, 2018.

Walters J, De luliis G, Nixon B, Bromfield E. Oxidative Stress in the male germline: A review of novel strategies to reduce 4-hydroxynonenal production. **Antioxidants.** 7(10): 132, 2018.

5. Oxidative stress associated with proteomic and fatty acid profiles of sperm from Nellore bulls at rest.

Camilo José Ramírez-López[1,3]*, Edvaldo Barros[2], Pedro Marcus Vidigal[2], Denise Okano Silva[1], Lidiany Lopes Gomes[1], Rener Philipe Rodrigues Carvalho[3], Alex Gazolla de Castro[4], Maria Cristina Baracat-Pereira[5], José Domingos Guimarães[1], Simone Eliza Facioni Guimarães[6]

[1]Animal Reproduction Laboratory, Universidade Federal de Viçosa, Brazil.

[2]Nucleus for Analysis of Biomolecules, Universidade Federal de Viçosa, Brazil.

[3]Structural Biology Laboratory, Universidade Federal de Viçosa, Brazil.

[4]Biotechnology and Biodiversity for the Environment Laboratory, Universidade Federal de Viçosa, Brazil.

[5]Proteomics and Protein Biochemistry Laboratory, Universidade Federal de Viçosa, Brazil.

[6]LABTEC-Animal Biotechnology Laboratory, Universidade Federal de Viçosa, Brazil.

Corresponding author: camilo.lopez@ufv.br

ABSTRACT:

Background: Sexual rest is a transient condition that some bulls have and can compromise conception rates in bovine herds, characterized by large volumes of ejaculate with high percentages of dead sperm. The mechanisms that lead to this sperm pattern are not clear, however, they seem to be related to the oxidative status of spermatozoa. **Methods:** Six adult Nellore bulls were submitted to Breeding Soundness Evaluation and fourth consecutive semen collections by the electroejaculation method in a period of 30 min. For each ejaculate, the

phenotypic parameters of the semen were evaluated. Aliquots of spermatozoa from the first and fourth ejaculate were used to determine the enzymatic activity of superoxide dismutase, catalase and glutathione S-transferase. Malondialdehyde and nitric oxide concentrations were determined as markers of lipid peroxidation. fatty acid profile and proteomics were also analyzed by GC-FID and LC-MS/MS respectively. **Results:** All sperm parameters showed a difference between the first and fourth ejaculate. Spermatozoa from the first ejaculate showed lower enzymatic activity and higher concentration of lipid peroxidation markers. Nineteen fatty acids were identified, 52.7% of which were polyunsaturated. Relative abundance analysis showed that C12:0 and C18:0 fatty acids differed between groups, being higher in spermatozoa from the fourth ejaculate. A total of 974 proteins were identified in both sample groups. Functional classification showed that most of the identified proteins were related to Cellular Processes and Signaling. Quantitative proteomics showed 36 differentially abundant proteins, six up-regulated proteins in the first ejaculate and 30 up-regulated proteins in the fourth ejaculate. **Conclusions:** spermatozoa from bulls at sexual rest have less antioxidant capacity, causing changes in their fatty acid composition and protein profile, which generates the observed sperm pattern and lower fertilization capacity.

Keywords: Spermatozoa, bovine, lipid peroxidation, lipid, proteins**.**

5.1. INTRODUCTION

Reproductive efficiency is the factor with the greatest economic impact on animal production, as it is a complex characteristic involving genetics, health, management, and nutrition, and requires knowledge to obtain maximum animal performance[1-4]. The development of biotechnologies applied to reproduction has contributed to the genetic advance registered in recent years in world livestock, however, there is no technology capable of obtaining results similar to those obtained in the natural mating system[5-8].

The selection of breeding bulls with proven fertility is essential to ensure sustainability and economic return to cattle breeding[9]. Due to the complex nature of the events involved with the fertilizing capacity of spermatozoa, several situations or conditions can influence the competence and integrity of sperm cells, resulting in reproductive failure of bulls and economic losses in beef cattle[10-12]. One of these conditions is the use of reproductives in sexual rest (SR), which due to the presented sperm parameters, the short periods of the breeding seasons, and the interval between the estrus of the matrices, can compromise the pregnancy rates[13, 14]. Additionally, SR can be a reason for discarding breeding bulls, especially when the andrologist is not familiar with changes in sperm parameters typical of SR.

SR is a condition or stage that some bulls have after going through a period of sexual inactivity and is characterized by the accumulation of senile spermatozoa in the extragonadal ducts such as the tails of the epididymis and the ampullae of the vas deferens[15]. The ejaculates of bulls in SR are characterized by having a large volume, low or no sperm motility, high cell concentration, and a high percentage of dead and decapitated sperm [15]. The accumulation of spermatozoa does not seem to have a defined etiology, however, it may be related to alterations in the stimulation mechanisms of the smooth muscle fibers of the epididymis responsible for

the displacement of spermatozoa through the epididymal ducts or with changes in the pH of the tail of the epididymis, increasing the metabolic rate and the accumulation of toxins[16,17].

Although the macroscopic characteristics of the ejaculates of bulls in SR are well-defined, the molecular alterations resulting from the accumulation of spermatozoa remain unclear. Some hypotheses suggest that sperm aging, as a consequence of the accumulation of extra gonadal reserves, favor the establishment of a state of oxidative stress due to the inversely proportional relationship between the production of reactive oxygen species (ROS) and the depletion of sperm antioxidant systems, resulting in the degradation of fatty acids (FA) in plasma membranes, loss of fluidity and flexibility of sperm membranes, protein dysfunction, and formation of toxic products that irreversibly culminate in cell death[18-22].

Although, high amounts of ROS are implicated in several processes that cause male infertility, in low or moderate amounts, ROS play an important role in sperm physiology as mediators of sperm capacitation, hyperactivation of motility and the acrosomal reaction through the activation of cascades signals modulated by protein phosphorylation[23].

Given this scenario, it seems key to determine the status of oxidative stress in spermatozoa from bulls at rest as a first step to understanding the molecular changes caused by this condition on sperm viability. Thus, our purpose with this work was to determine a possible relationship between SR and the onset of oxidative stress in spermatozoa of adult Nellore bulls as a first measure to understand the sperm characteristics presented by sires under this condition and its effects on sperm composition of FA and the proteomic profile of spermatozoa.

5.2. RESULTS

Sperm analysis from Nellore bulls in sexual rest:

It was necessary to carry out four consecutive semen collections to obtain sperm parameters compatible with reproductive fitness in bulls in SR (Table S1). All semen phenotypic characteristics evaluated in this study showed differences between the first and fourth ejaculate ($p<0.05$). Sperm parameters Mass Motility, Motility and Vigor exhibited an ascending pattern in their mean values, at each semen collection performed due to the reestablishment of reproductive fitness. Conversely, sperm concentration, volume, aspect and the percentage of total sperm defects in the ejaculates showed a descending pattern at each semen collection, as a result of sperm depletion of extragonadal reserves (Fig. 1). The isolated normal head (decapitation without anatomical alterations) was the most observed sperm defect in bulls with RS, followed by acrosome and tail defects. We emphasize that all of the acrosome defects observed in our study corresponded to edematous acrosome. Based on the results of sperm analyses, we only considered spermatozoa from the first and fourth (last) ejaculate to carry out subsequent analyzes as they constituted the two most contrasting moments.

Oxidative stress status of spermatozoa from Nellore bulls in sexual rest:

Superoxide dismutase (SOD), Catalase (CAT), and Glutathione-S-transferase (GST) enzymes showed higher activity in the fourth ejaculated sperm whose sperm parameters showed values compatible with reproductive fitness ($p<0.05$). However, lipid peroxidation determined by malondialdehyde (MDA) concentration and Nitric oxide (NO) levels were higher in sperm from the first ejaculation where the percentage of motility was lower and sperm defects were higher (Fig. 2).

Fatty acid profile of spermatozoa from Nellore bulls in sexual rest:

The analysis of FAs in the sperm cells of bulls in SR by gas chromatography allowed the identification of 19 FA. Of these, 47.3% are saturated FA and 52.7% unsaturated,

corresponding to 40% monounsaturated and 60% polyunsaturated (PUFAS). Proportionally, spermatozoa from the first ejaculate had a higher percentage of unsaturated FA while spermatozoa from the fourth ejaculate had a higher amount of saturated FA. The presence/absence analysis revealed four FAs (C15:1 isoH/13:0 3OH, C16:0 2OH, C19:0, C20:0) present only in sperm from the first ejaculate and one FA (C10:0) present exclusively in sperm from the fourth ejaculate (Table S2). Relative quantification analysis showed a heterogeneous pattern in the abundance of FAs between the two sample groups. Despite this, differences ($p<0.05$) were observed in the percentage of FA C12:0 and C18:0, being higher in spermatozoa from the fourth ejaculate (Fig. 3).

Proteomic analysis of spermatozoa from Nellore bulls in sexual rest:

Using LC-MS/MS we identified 974 proteins in sperm from bulls in SR (Table S3). Among them, 123 proteins were identified exclusively in spermatozoa from the first ejaculate, while 116 proteins were identified solely in spermatozoa from the fourth ejaculate (Fig. 4). Based on the functional classification by KOG, the most predominant classes within the category of Cellular Processes and Signaling related to sperm proteins were Posttranslational modification, protein turnover, chaperones followed by Cytoskeleton and Signal transduction mechanisms (Fig. 5). Considering the importance of energy metabolism in the sperm cell and especially in spermatozoa stored for a prolonged period in extragonadal sperm reserve sites, the number of proteins classified in the Energy production and conversion, Lipid transport and metabolism and Carbohydrate transport and metabolism classes also stood out (Table S4).

The label-free quantification analysis of the identified proteins revealed 36 differentially expressed proteins (DEP) between the first and fourth ejaculate of bulls in SR, with six proteins being more abundant in the first ejaculate (*Serine/threonine-protein phosphatase, EF-hand domain-containing protein 1, Beta-galactosidase, Tissue alpha-L-fucosidase, Inactive*

serine/threonine-protein kinase VRK3, AMP-binding domain-containing protein) and 30 proteins in the fourth ejaculate (Fig. 6). Based on KEGG pathway analyses, DEP participate in several processes such as galactose metabolism, FA synthesis and degradation, oxidative phosphorylation and regulation of actin cytoskeletal (Table S5).

5.3. DISCUSSION

Our study is the first to provide evidence of the establishment of an oxidative stress state in sperm from bulls in SR and its consequences on FA composition and sperm protein profile. The results of our sperm analysis indicate that SR can compromise pregnancy rates in bovine herds managed by a controlled natural mating system. In addition, we verified the reversible character of RS, where the pattern exhibited by characteristics such as motility and sperm morphology, mainly in the first ejaculates, are products of prolonged accumulation and subsequent aging of spermatozoa and not as a result of changes in spermatogenesis.

Prolonged storage in the extragonadal reverse and subsequent aging of sperm predisposes the accumulation of cellular damage caused by the establishment of oxidative stress due to the neutralization of the main constituents of the antioxidant defense system by the excessive production of ROS and the limited capacity of cellular repair of spermatozoa[24]. The sperm antioxidant system is composed, among other molecules, of SOD, CAT, and GST enzymes that act by inhibiting ROS through different chemical reactions. SOD catalyzes the superoxide anion through the dismutation reaction, in hydrogen peroxide, which in turn, is degraded into oxygen and water by the action of CAT[25]. For its part, GST constitutes the main detoxification pathway of the second phase of the antioxidant defense and plays a fundamental role in protecting against lipid peroxidation (LPO), through the reduction of hydroperoxides and 4-hydroxynonenal, interrupting LPO and reducing the lipid oxidation damage[26].

LPO is an important cause of injury and cell death triggered by oxidative stress and occurs through chain reactions that lead to the collapse of plasma membranes and the loss of selective permeability, reducing sperm viability and the capacity for interaction between sperm and the oocyte[27]. The induction of LPO as a consequence of high levels of ROS generation accompanied by low antioxidant enzymatic activity, as observed in spermatozoa from the first ejaculate, culminate in the formation of lipid aldehydes and free radicals such as MDA and NO[28]. These by-products can spread to other cellular compartments, attacking proteins and DNA, and in the case of spermatozoa, they can also inhibit sperm motility due to their ability to covalently bind to the nucleophilic centers of proteins in the electron transport chain, causing the first place instances the interruption of mitochondrial electron transport and subsequently the increase in the efflux of electrons that associated with oxygen molecules and generated the superoxide anion, further intensifying the oxidative reaction and decreasing the synthesis of ATP[29].

Spermatozoa are cells particularly susceptible to LPO due to the high concentration of FAs in their plasma membranes, acquired during the process of cell differentiation in the testes and epididymal maturation[30]. ROS can abstract hydrogen molecules from the hydrocarbon side chains of FAs, forming lipid radicals. These lipid radicals are usually stabilized by molecular rearrangement, forming conjugated dienes[31]. Under aerobic conditions, lipid radicals react with oxygen molecules and form the peroxyl radical. The peroxyl radical is capable of abstracting hydrogen from adjacent lipid molecules and self-perpetuating the reaction. The combination of hydrogen with the peroxyl radical generates lipid hydroperoxides that undergo breakdown and form aldehydes such as MDA[32]. All these oxidative modifications cause changes in the physical and chemical properties of the membranes, altering their fluidity and permeability, and increasing the risk of rupture of membranes and organelles, with a

consequent increase in sperm abnormalities, loss of motility, and cell death[33]. Facts that may explain the high percentages of dead and decapitated sperm observed in the first ejaculates of bulls in SR.

FAs play important roles in cellular mechanisms, whether as a structural part of membranes, as a source of energy, or as signaling molecules[33]. Currently, there is enough scientific evidence demonstrating the relationship between FA and sperm quality parameters[35 - 37]. PUFAs constitute the main class of FA in sperm and are directly related to sperm motility by regulating the fluidity and flexibility of the plasma membrane of the sperm tail[38]. Despite this, a high proportion of PUFAs may be a predisposing factor for oxidative stress because they constitute the main substrate for LPO[39]. Saturated FAs, such as C12:0 (lauric acid) and C18:0 (stearic acid), were more resistant to LPO due to the absence of carbon double bonds in their structural chains[40]. Indeed, high concentrations of lauric acid and stearic acid were positively correlated with sperm viability and motility in stallions classified as good freezers and healthy donkeys, respectively[41-42]. Studies with porcine and bovine semen suggest that long-chain saturated FA can preserve sperm motility and viability by keeping ROS levels low and constituting an energy substrate for ATP production via β-oxidation[43-44]. Although glycolysis and oxidative phosphorylation constitute the main energy generation pathways used by spermatozoa, Zhu et al. 2019[45], reported that sperm cells can use different metabolic pathways to generate ATP depending on the substrate of the microenvironment where they are found to maintain motility, thus justifying the proposition of using the β-oxidation pathway by spermatozoa.

The formation of MDA as a consequence of LPO can modify proteins through oxidation of their thiol groups and carbonylation, resulting in cellular dysfunction and activation of the apoptotic cascade[46]. In this context, the sperm proteins *Midkine, Cathepsin L2, Prosaposin,*

S100 calcium binding protein A9, Annexin, Metalloproteinase inhibitor 2 and *Nucleobindin-1* involved in processes such as the ability of sperm to overcome the barriers formed by cumulus cells, binding to the zona pellucida, fertilization and embryonic development showed low abundance in the spermatozoa of the first ejaculate, evidencing the incompetence of these spermatozoa in fulfilling their functions[47-50]. *Midkine* is a heparin-binding protein that interacts with the glycosaminoglycans of the *cumulus-oophorus* complex, facilitating the binding of sperm to the oocyte. Additionally, *Midkine* exhibits anti-apoptotic effects and promotes sperm migration and survival[51-52].

For their part, *Metalloproteinase inhibitor 2* and *Nucleobindin-1*, in addition to participating in the interaction between gametes, are involved in the remodeling of the extracellular matrix, responsible for providing a tissue support structure and favoring communication between embryonic cells and their microenvironment, interaction that is transcendental to embryonic implantation [53].

According to the results of the quantitative proteomics analysis, the antioxidant capacity mediated by sperm proteins was also compromised by SR. Proteins such as *Albumin, Ribonuclease 4, Hemoglobin beta, Hemoglobin subunit alpha, Spemadhesin-1* and *Vanin 2* protect spermatozoa from injuries caused by excess ROS through different mechanisms, showing low abundance in spermatozoa of the first ejaculate[54-55]. *Albumin* cause a reduction in hydrogen peroxide formation and absorbs lipid peroxides, having a protective effect on both the membrane and sperm motility[50]. While *Vanin 2* has pantetheinase activity, involved in the hydrolysis of pantetheine to generate pantothenic acid (vitamin B5) and cysteamine[56]. Pantothenic acid and cysteamine play an important role in cellular protection against oxidative damage as they are precursors of glutathione, one of the most potent intracellular antioxidants [57].

Spermadhesin-1 has an indirect protective effect against oxidative stress by reducing the mitochondrial metabolism of sperm stored in extragonadal reserves through its binding to phospholipids, carbohydrates and membrane glycosaminoglycans[58]. Precisely, its great binding capacity to different ligands grant Spemadhesin-1 the ability to act as a decapacitating and preventive agent of spontaneous acrosome reaction (ARs)[59]. ARs is a phenomenon characterized by presenting sperm populations with the acrosome reacting prematurely, causing a decrease in the fertilizing capacity of sperm due to the impossibility of penetrating the *cumulus-oophorus* and encountering into contact with the zona pellucida[60-61]. The causes that trigger RAs are multifactorial and unclear, however, prolonged exposure to ROS due to excessive storage in organs of the reproductive system seems to be one of the main causes[62].

Sperm has some intrinsic mechanisms to predict ARs, one of which is the polymerization of actin filaments during capacitation, which prevents swelling of the outer acrosomal membrane and its fusion with the plasma membrane[63]. Actin polymerization is mediated by two pathways, activation of *Phospholipase D* (PLD) and *Ca2+/calmodulin-dependent protein kinase II* (CaMKII). Both pathways are dependent on *Protein kinase A* (PKA) and converge on the cross-linkers activity that *Ezrin* protein exerts between the plasmatic membrane and the actin filaments[64].

During the activation process of the CaMKII pathway, PKA activates the enzyme *sarcoma-tyrosine kinase*, which in turn inhibits *Serine/threonine-protein phosphatase* and activates CaMKII, causing actin polymerization[65]. Thus, *Serine/threonine-protein phosphatase* and *Ezrin* play a crucial role in the prevention of ARs. Precisely, these two proteins were identified with low and high abundance in sperm from the first ejaculate, respectively. The abundance pattern of *Ezrin* and *Serine/threonine-protein phosphatase* in our work suggests that SR can induce ARs in bovine sperm probably by prolonged exposure to ROS.

The high abundance of *Tissue alpha-L-fucosidase* in first ejaculate spermatozoa constitutes further evidence on the inductive role of SR in ARs, because *Tissue alpha-L-fucosidase* is an enzyme located within crypts in the outer acrosomal membrane and its increase in spermatozoa is related to their release during the exocytosis that occurs in the acrosome reaction[66].

Changes in oxidative status can lead to cell death due to an ionic imbalance. In fact, hydrogen peroxide activates the protein *Transient Receptor Potential M2* (TRPM2) through vi β-NAD and ADP-ribose, which acts as a permeable cation channel for calcium and increases its intracellular concentrations[67]. It was observed that the expression of *EF-hand domain-containing protein 1*, a protein that is differentially abundant in spermatozoa from the first ejaculate, potentiates the action of the TRPM2 transporter due to its regulatory function of the transit of molecules through membrane channels, causing dyshomeosthesis of calcium and cell death in neurons[68].

Despite the evidence demonstrating the involvement of EF-hand domain-containing protein 1 in mechanisms that lead to cell death, our analyzes do not allow us to assert its implication in the death of spermatozoa from bulls in SR, requiring specific tests to confirm our speculation.

In addition to describing the physiological changes of spermatozoa in SR, our results also demonstrate great applicability in the cattle breeding sector, as we show how a simple change in the management of bulls in SR can decrease the rate of breeding culling and reduce animal replacement costs within the herd. Additionally, we emphasize that a single semen collection in some cases is not enough to assess the true reproductive potential of the bulls and each case must be treated individually to make the appropriate diagnosis.

5.4. CONCLUSIONS

Our results indicate that oxidative stress may be related to sperm characteristics observed in Nellore bulls at sexual rest. Prolonged exposure to reactive oxygen species due to accumulation in extragonadal reserves probably causes a low percentage of sperm motility since high concentrations of lipid peroxidation by-products can alter some metabolic pathways used by spermatozoa for energy generation. Our results also indicate that under oxidizing conditions, sperm fatty acid composition may be related to the increase in the percentage of sperm defects due to reduced fluidity and permeability of the plasma membrane. In addition, oxidative stress can modify the proteomic profile of spermatozoa and compromises their viability since several proteins related to the fertilizing capacity showed low abundance in the spermatozoa of the first ejaculate.

5.5. Methods

Ethics approval

This study was submitted and approved by the Ethics Committee for the Use of Animals of the Universidade Federal de Viçosa (proc. n 60/2019). All methods were carried out by relevant guidelines and regulations, and all methods are reported by the ARRIVE guidelines (https://arriveguidelines.org).

Selection of animals

Six adult Nellore bulls were selected in sexual rest condition through Breeding Soundness Evaluation and submitted to consecutive semen collections by the electroejaculation method until reaching sperm parameters compatible with reproductive fitness according to the criteria established by the Colégio Brasileiro de Reprodução Animal[69]. All bulls were nutritionally managed on tropical pastures (*Brachiaria brizantha*) and were sexually inactive

for at least six months. All collections were performed on the same day and with an interval of 10 minutes between total collections. At the time of the Breeding Soundness Evaluation, the reproductive organs were examined and the scrotal perimeter of all bulls was measured using a tape measure in the widest region of the scrotum[70]. After each collection, the volume (mL), physical aspect (1: aqueous, 2: opalescent, 3: milky, 4: creamy), and sperm concentration of each ejaculate in a Neubauer camera were determined and the physical characteristics of the semen were evaluated, estimating mass motility (on a scale of 0 to 5), sperm motility (%) and sperm vigor (on a scale of 0 to 5), in an aliquot of semen analyzed in conventional optical microscopy (CX31, Olympus, Tokyo, Japan). Morphological characteristics were evaluated in wet preparation, between slide and coverslip at 1000x magnification under immersion in phase contrast microscopy (BX41, Olympus, Tokyo, Japan). For each preparation, 200 cells were counted, and the percentage of spermatozoa with defects in the acrosome, head, intermediate piece, and tail. Subsequently, pathologies were classified into major, minor, and total defects[71].

After evaluating semen characteristics, ejaculates were centrifuged at 700*g* for 10 min to separate sperm from seminal plasma. Sperm from the first and last ejaculation of each bull were stored in 0.5 mL straws and stored in liquid nitrogen at -196°C until the day of analysis.

Sample preparation for oxidative stress analysis

To obtain the intracellular content of sperm from the first and last ejaculate of each bull, 100 µl aliquots were subjected to five repetitions of freezing in liquid nitrogen and subsequent incubation in an ultrasound bath for 15 min to extract the proteins . After these procedures, the samples underwent centrifugation at 10,000*g* (4 °C) for 10 min. The protein content in the supernatant was assessed by the Bradford method[72] and, used to normalize the activity of antioxidant enzymes. Superoxide dismutase (SOD) activity was evaluated by the pyrogallol method as described by Dieterich et al. (2000)[73]. Catalase activity was evaluated by measuring

the kinetics of hydrogen peroxide decomposition according to the methodology of Aebi (1984)[74]. Glutathione-S-transferase (GST) activity was determined from the NADPH oxidation rate as described by Habig et al., (1974)[75]. Nitric oxide (NO) was determined indirectly by quantifying nitrite/nitrate levels according to the Griess methodology[76]. Lipid peroxidation was evaluated in the analysis of malondialdehyde (MDA) levels by incubation with thiobarbituric acid to assess the levels of substances reactive to thiobarbituric acid[77].

Sample preparation for fatty acid (FA) analysis

The FAs were analyzed from 100 µl aliquots by gas chromatography according to Corradini et al., 2014 [78]. Briefly, the FAs were processed for direct transesterification with acetyl chloride, then added with methyl pentadecanoate as an internal standard and the identification, Precision, and accuracy were assessed using mixtures of FA standards. Analyzes were performed on a gas chromatograph (Agilent 6890 GC Series, Agilent Technologies, Santa Clara, USA), equipped with an automatic liquid sampler and a flame ionization detector (GC-FID). Separation was performed on a 199 µm x 0.33 µm capillary column (Agilent, 19091B-102, 199 µm, Agilent Technologies, Santa Clara, USA).

Sample preparation for proteomic analysis

Aliquots of 100 µl spermatozoa from the first and last ejaculate of each bull were lyophilized (L101, Liobras, São Paulo, Brazil), and resuspended in 1 mL of 4% CHAPS solution (3-3-cholamidopropyl dimethylammonium-1-propane sulfonate). Then, the samples were submitted to an ultrasonic bath (USC 1880, Unique, São Paulo, Brazil) for 15 min and centrifuged (Heraeus Multifuges X1R, Thermo Scientific, Waltham, USA) at 10,000*g* at 4°C for 10 min. The supernatant was transferred to a new tube and proteins were quantified by the Bradford method[72].

An aliquot of each sample containing 50 µg of protein was analyzed by one-dimensional electrophoresis (SDS-PAGE). SDS-PAGE was performed by running the gel in two stages (splitting: 14% T, 3.0% C, stacking: 5.1% T, 2.6% C) at 80 V for 15 min and 60 V for 4 h, using the Mini-PROTEAN Tetra Cell equipment (Bio-Rad, Hercules, USA). At the end of the run, the gels were stained with Coomassie Brilliant Blue R-250 (Bio-Rad, Hercules, USA) for 2 h and destained for 10 h in a solution of methanol 25% (v/v) and 7.5% (v/v) acetic acid[79].

After analysis of the protein profile separated by SDS-PAGE, two pools of samples were formed consisting of spermatozoa from the first and last ejaculate of each bull. Then, five replicates from each pool containing 50 µg of proteins per replicate were immobilized and concentrated by SDS-PAGE Shor-Run strategy (split: 12.5% T, 3.0% C, stacking: 4.0% T, 2.6% C) using the Mini-PROTEAN Tetra Cell apparatus (Bio-Rad, Hercules, USA)[80]. The electrophoresis process took place under a constant 80 V, which was stopped when the bromophenol blue indicator reached about 10 mm from the top of the separation gel. After the run, the gels were cut into two parts, which were placed in a fixative solution (40% (v/v) methanol and 5% (v/v) acetic acid) for 2 h. Then, one of the parts was stained in a Coomassie Brilliant Blue R-250 staining solution (Bio-Rad, Hercules, USA) for approximately 2 h.

Gel protein digestion

The bands from the SDS-PAGE Short-run were excised, cracked, and subjected to enzymatic digestion[81]. Briefly, the gel fragments were placed in microtubes containing 200 µL of 50% (v/v) acetonitrile (ACN) in 25 mM ammonium bicarbonate (pH 8.0) and subjected to washes to remove dye and SDS. Then, the dehydration of the gels was performed by adding, twice, 200 µL of 100% ACN in each microtube, keeping them at rest for 5 min.

The proteins present in the fragments of the gels were reduced and alkylated in DTT and iodoacetamide respectively. Subsequently, the gel fragments were washed, hydrated, and

dehydrated twice with ammonium bicarbonate and ACN, and finally dried in a vacuum concentration system (Concentrator Plus AG - 22331, Eppendorf, Hamburg, Germany).

The gel fragments were digested using 100 µL of porcine pancreas trypsin solution (Sigma-Aldrich, Burlington, USA), at a final concentration of 25 ng/µL in activation solution (40mM ammonium bicarbonate (pH 8.0) and 10% (v/v) ACN) and left in a water bath at 37ºC for 22 h. After proteolysis, the tryptic peptides were removed in a solution of 5% (v/v) formic acid in 50% (v/v) ACN, concentrated in a vacuum centrifuge system, and desalted using C18 reversed-phase micro columns (ZTC18S096, Millipore, Burlington, USA) and eluted in a 50% ACN solution, acidified with 0.1% (v/v) trifluoroacetic acid.

Mass spectrometry

The constituent peptides of the samples were solubilized in 20µL of 0.1% (v/v) aqueous formic acid solution, with the addition of 2% (v/v) ACN. Subsequently, 1 µL of the solution was analyzed by nano LC-MS/MS system using an ultra-high performance liquid chromatograph - UHPLC NanoAcquity (Waters, Milford, USA), containing a trap column model nanoAcquity UPLC® 2G-V/MTrap 5µm Symmetry® C18 180 µm x 20 mm at a flow rate of 7 µL/min for 3 min. Peptides were separated using a nanoAcquity UPLC® 1.8 µm HSS T3 75 µm x 200 mm column, operating with a flow rate of 0.2 µL/min. The mobile phase of the chromatographic process used water acidified with 0.1% formic acid (solvent A) and ACN acidified with 0.1% formic acid (solvent B) as solvents. Chromatographic separation occurred according to the following schedule: 2% B for 1 min, gradient from 2% to 30% B over 209 min, gradient from 30% to 85% B for 10 min, maintenance at 85% B for 5 min, gradient from 85% to 2% B for 5 min, and maintenance in 2% B for 10 min, totaling 240 min of chromatographic analysis.

The eluted peptides were automatically injected into a MAXIS 3G model mass spectrometer (Bruker Daltonics, Billerica, USA), operating in online mode, with a CaptiveSpray ionization source. Peptides analyzis was done by an appropriate method for proteomic analysis (IE_captive_nov2019), with a drying gas flow of 3L/min, ionization source temperature of 150ºC, and transmission voltage of 2 kV. The raw data were converted into a list of masses in the *mzXML extension (Extensible Mark-up Language), using the CompassXport application, version 3.0 (Bruker Daltonics, Billerica, USA), which was submitted to identification using the PEAKS software.

Analysis of data from mass spectrometry

Lists of masses with the *mzXML extension were compared against the Bovidae protein database (Taxonomy ID 9895) deposited in the UniProt Knowledgebase database (UniProtKB, https://www.uniprot.org/, accessed on 03-31- 2022).

The comparison was performed using the PEAKS application, version 7.0 (Bioinformatics Solutions Inc., Ontario, Canada)[82]. The parameters used for the research were: enzymatic digestion by trypsin not considering the occurrence of lost cleavage, cysteine carbamidomethylation as a fixed modification and methionine oxidation as a variable modification. Error tolerance for the parent ion of 20 ppm and 0.6 Da for the fragments, considering the analysis of ions with charges +2, +3, and +4. Proteins were considered identified when they presented at least two unique peptides with FDR (False Discovery Rate) lower than 1%.

Proteins identified by PEAKS as “Uncharacterized” were analyzed using BLAST software, version 2.4.0[83]. In this analysis, it was possible to identify which proteins deposited in the NCBI protein non-redundant (nr) database showed greater identity with the sequences of the “Uncharacterized” proteins.

For the label-free quantification analysis, the peak areas of the proteins identified in the three technical replicates with the highest correlations among themselves per group were considered. Acceptance parameters were: a -10 Log P score of 20 (equivalent to a p-value of 0.01), a fold change > 1.5, and an FDR < 1%[84].

Functional classification of proteins

Identified proteins were classified by the RPSBLAST tool of BLAST version 2.13.0 [82] into categories from the EuKaryotic Orthologous Groups (KOG) database [85], using an E-value threshold of 1e-10 to select significant alignments. Differentially abundant proteins were annotated in the KEGG pathway database (http://www.genome.jp/kegg/pathway. html). The analysis was performed using the freely available BlastKOALA (http://www.kegg.jp/blastkoala/) sequence similarity tool.The annotated proteins obtained from the KEGG database were categorized based on their functional roles[86].

Statistical Analysis

Differences between semen physical characteristics were evaluated in the four moments by the Friedman test, followed by the Dunn-Bonferroni test. The data relating to the analysis of oxidative stress were submitted to the paired t-test after verification of normality by Shapiro-Wilk. For all tests, a significance level of 5% was considered.

5.6. Figures

Figure 1. Seminal characteristics of Nellore bulls at rest and during sexual activity. Medians and interquartile ranges of ejaculates and sperm quality parameters. MOT: Sperm Motility; VIG: Sperm Vigor; DefT: Sperm Total Defects; Con: Sperm Concentration; Asp: Ejaculate Aspect; MM: Sperm Mass Motility; Vol: Ejaculate Volume. *p<0,05; **p<0,01;

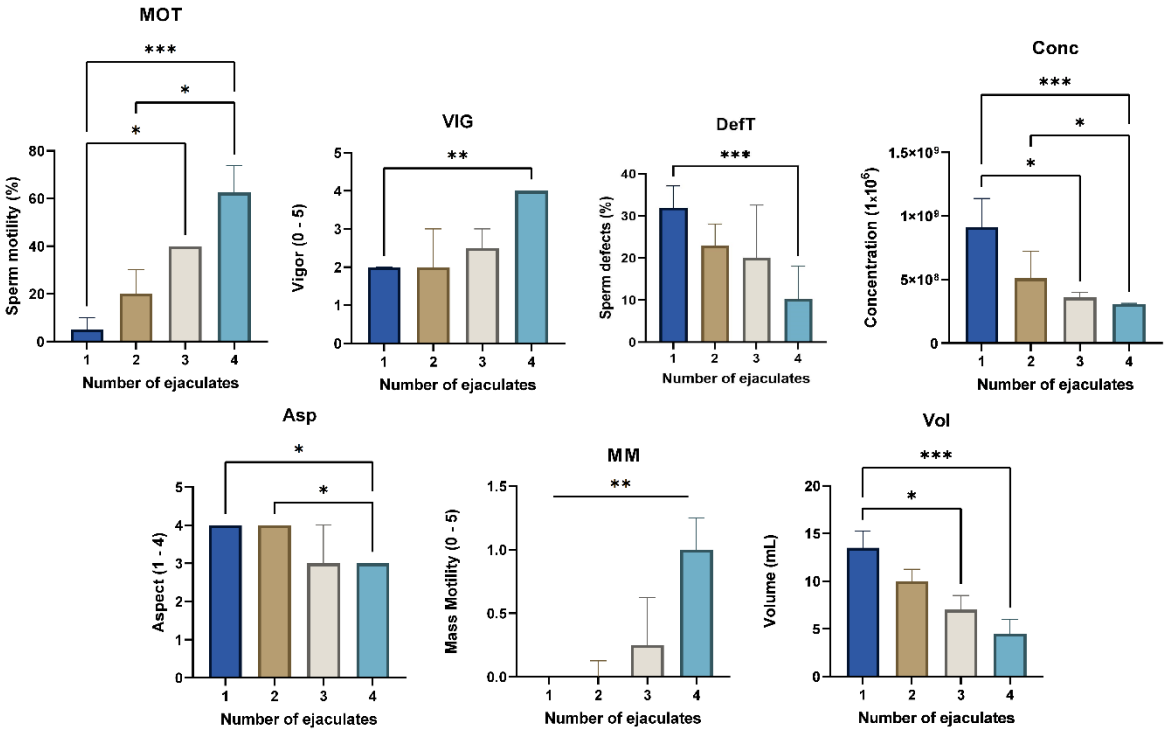

***p<0,001.

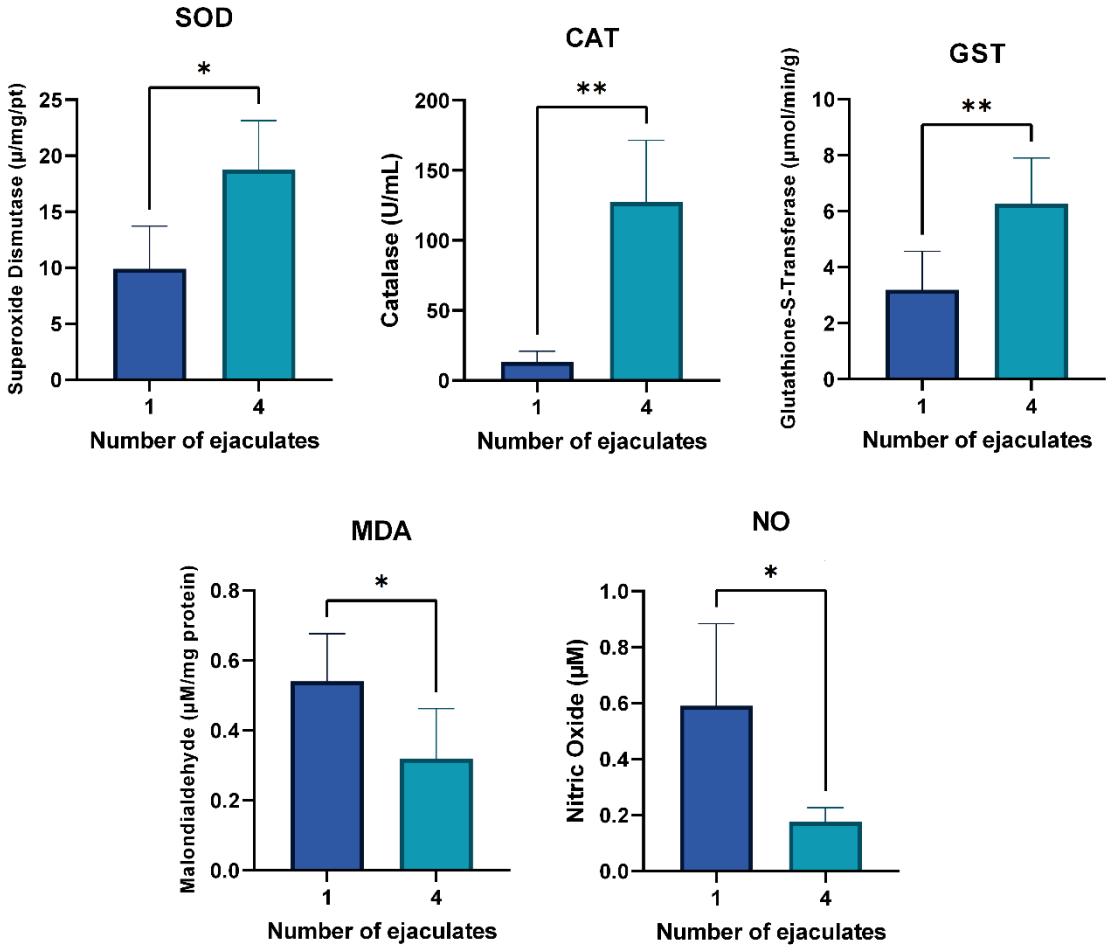

Figure 2. Antioxidant enzyme activity and oxidative/nitrosative stress markers in sperm extract from Nellore bulls at rest and during sexual activity. The column represents the mean value; whiskers represent the maximum data. Superoxide Dismutase; CAT: Catalase; GST: Glutathione-S-Transferase; MDA: Malondialdehyde; NO: Nitric Oxide. *p<0,05; **p<0,01.

.

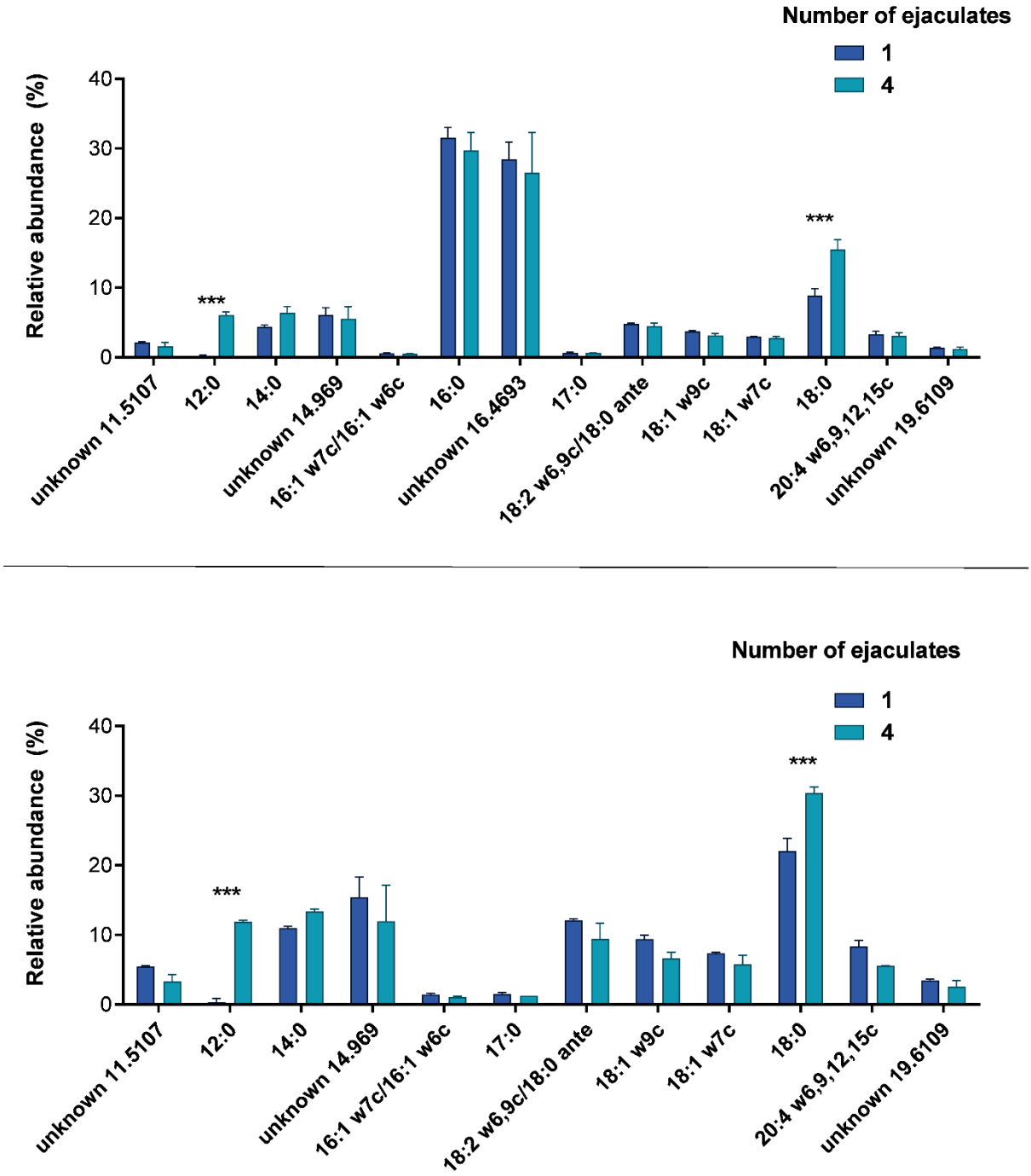

Figure 3. Relative abundance of Fatty Acids identified in sperm extract from Nellore bulls at rest and during sexual activity. A: relative quantification of total FA identified; B: relative quantification of FA excluding the most abundant. The column represents the mean value;

whiskers represent the standard deviation. ***Significant difference ($p<0.001$) between ejaculates.

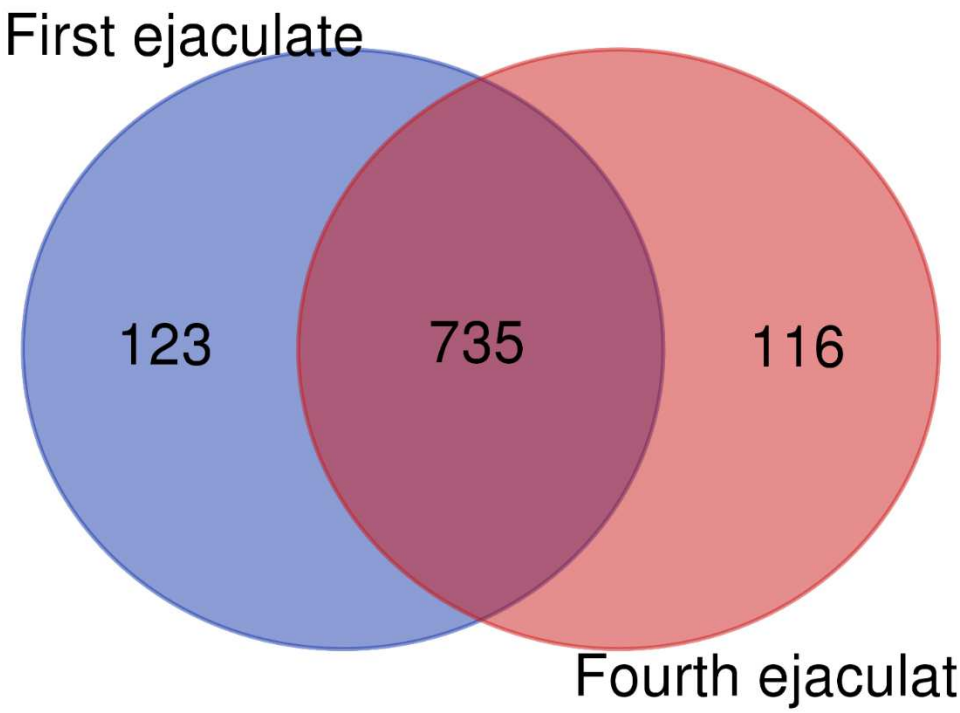

Figure 4. Proteomics profile of sperm extract from Nellore bulls at rest and during sexual activity. From the total of 974 proteins, 858 were identified in the spermatozoa of the first ejaculate (Group A) and 851 in the spermatozoa of the fourth ejaculate (Group B). The intersection shows 735 proteins conserved in both spermatozoa groups. Group A has 123 unique proteins while Group B has 116 unique proteins.

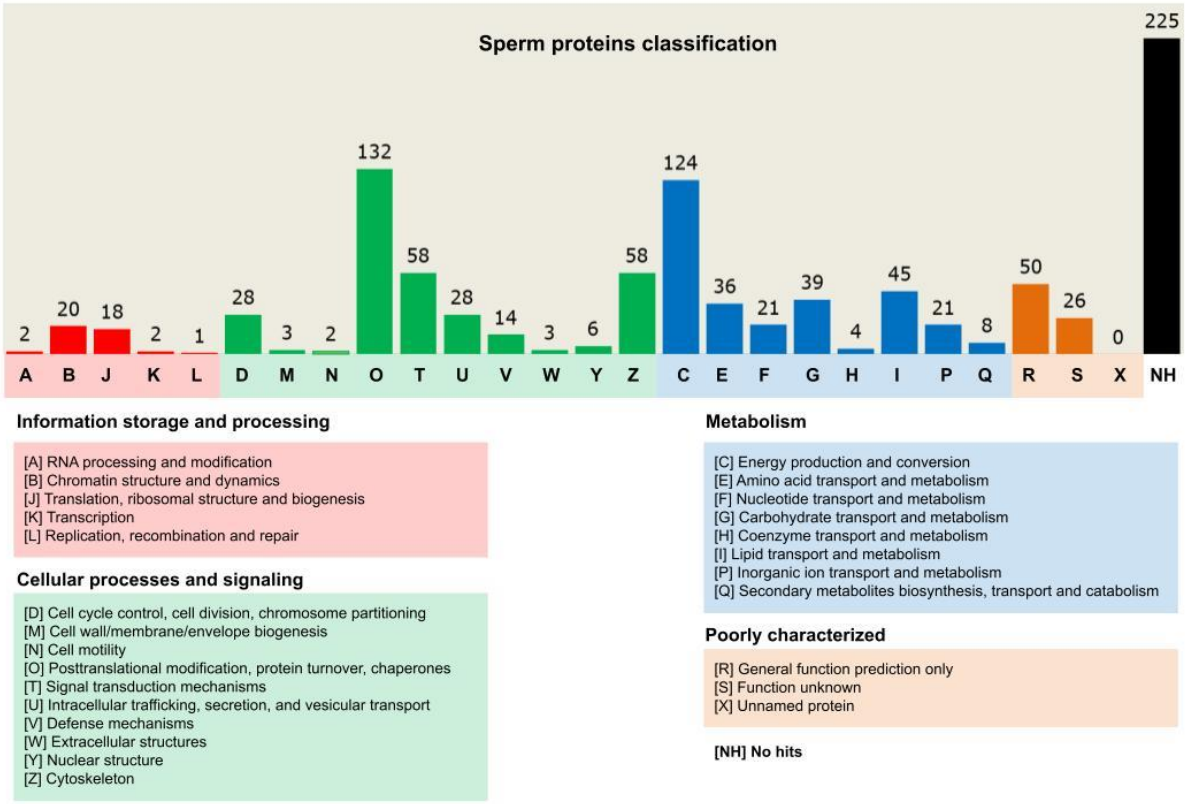

Figure 5. Functional classification of sperm extract proteins from Nellore bulls at rest and during sexual activity. The sequence similarity searches classified 749 proteins into four main groups of the KOG database. One hundred proteins did not show significant hits [NH] and were not classified. The twenty-six letters from [A] to [Z] represent the functional categories of the KOG database. “Posttranslational modification, protein turnover, chaperones” [O] and “Energy production and conversion” [C] were the categories with the highest number of annotated proteins.

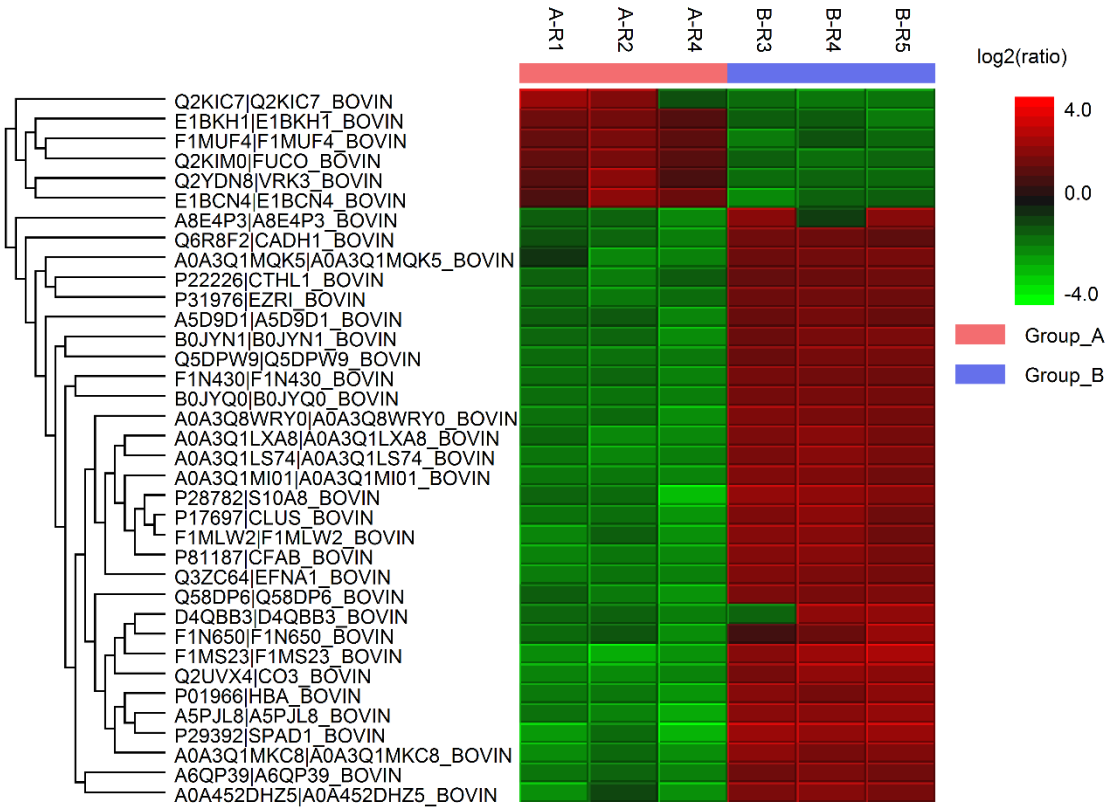

Figure 6. differentially abundant proteins in sperm extract from Nellore bulls at rest and during sexual activity. The label-free quantification analysis identified 36 differentially abundant proteins (DAP) in the spermatozoa of bulls in sexual rest. The heatmap shows the distribution of DAP abundance values in technical replicates. The colors represent the peak area values submitted to the row scale. Red squares indicate high abundance, and green squares indicate low one. Group A: spermatozoa first ejaculate; Group B: spermatozoa of fourth ejaculate

5.1.Tables

Table S1. Semen phenotypic parameters of Nellore bulls in sexual rest. Physical and morphological parameters of the semen of Nellore bulls collected by the electroejaculation method and evaluated by microscopy.

BULLS	CE (cm)	Volume (ml)				Mass Motility (0 - 5)				Motility (%)				Vigor (0 - 5)				Aspect				Concentration (1000,000 x ml)				Morphology (%)			
		A	B	C	D	A	B	C	D	A	B	C	D	A	B	C	D	A	B	C	D	A	B	C	D	A	B	C	D
Bull 1	41,7	16,0	12,0	8,0	4,0	0,0	0,0	0,5	1,0	5,0	20,0	40,0	65,0	2,0	2,0	2,0	4,0	4,0	4,0	3,0	3,0	722.500.000	657.500.000	390.000.000	305.000.000	37,0	26,5	20,0	12,5
Bull 2	40,5	15,0	10,0	6,0	4,0	0,0	0,0	0,0	1,0	0,0	20,0	40,0	60,0	0,0	2,0	2,0	4,0	4,0	4,0	4,0	3,0	1.257.500.000	925.000.000	417.500.000	312.500.000	33,5	33,0	30,5	18,5
Bull 3	43,4	12,0	8,0	6,0	3,0	0,0	0,0	0,0	0,0	0,0	20,0	40,0	70,0	0,0	2,0	2,0	3,0	4,0	4,0	3,0	2,0	782.500.000	422.500.000	342.500.000	132.500.000	30,5	20,0	12,5	8,0
Bull 4	40,3	12,0	8,0	4,0	5,0	0,0	0,5	1,0	2,0	5,0	20,0	40,0	60,0	2,0	3,0	3,0	3,0	4,0	4,0	3,0	3,0	980.000.000	410.000.000	322.500.000	307.500.000	21,0	14,5	12,5	7,0
Bull 5	39.8	12,0	10,0	10,0	6,0	0,0	0,0	0,5	1,0	10,0	30,0	40,0	60,0	2,0	3,0	3,0	4,0	4,0	4,0	4,0	3,0	842.500.000	467.500.000	375.000.000	312.500.000	37,5	24,0	39,0	6,0
Bull 6	44,5	15,0	11,0	8,0	6,0	0,0	0,0	0,0	0,0	10,0	30,0	40,0	85,0	2,0	2,0	3,0	4,0	4,0	4,0	3,0	2,0	1.097.500.000	552.500.000	340.000.000	192.500.000	30,5	22,0	20,0	18,0
		13,5	10,0	7,0	4,5	0,0	0,0	0,3	1,0	5,0	20,0	40,0	62,5	2,0	2,0	2,5	4,0	4,0	4,0	3,0	3,0	911250000,00	510000000,00	358750000,00	306250000,00	32,0	23,0	20,0	10,3

Table S2. Profile of Fatty acid in in sperm extract from Nellore bulls at rest and during sexual activity. Numeric abbreviation, trivial name, and a class of FA identified by GC-FID.

Peak Name	Trivial Name	FA Class	First ejaculate			Fourth ejaculate		
			A1	A2	A3	B1	B2	B3
15:1 iso H/13:0 3OH		Monounsaturated	0,00	0,25	0,23			
16:1 w7c/16:1 w6c	Palmitoleic acid	Monounsaturated	0,65	0,51	0,56	0,48	0,55	0,51
18:1 w9c	Oleic acid	Monounsaturated	3,67	3,71	3,84	2,89	3,41	3,17
18:1 w7c	Vaccenic acid	Monounsaturated	2,99	2,94	2,89	2,54	2,63	3,04
unknown 11.5107		Polyunsatured	0,00	2,22	2,07	1,10	2,16	1,53
unknown 14.969		Polyunsatured	5,96	5,24	7,18	5,54	3,76	7,28
unknown 16.4693		Polyunsatured	27,47	26,65	31,30	22,43	14,13	30,58
18:2 w6,9c/18:0 ante	Linoleic acid	Polyunsatured	4,89	4,90	4,69	4,05	4,25	5,02
20:4 w6,9,12,15c	Arachidonic acid	Polyunsatured	3,85	3,18	3,02	2,70	2,99	3,57
unknown 19.6109		Polyunsatured	1,45	1,33	1,39	1,03	1,11	1,49
10:0	Capric acid	Saturated				1,15	1,47	0,00
12:0	Lauric acid	Saturated	1,48	0,28	0,00	5,72	6,41	0,89
14:0	Myristic acid	Saturated	4,65	4,39	4,15	6,40	7,33	5,53
16:0	Palmitic acid	Saturated	31,21	33,16	30,31	28,84	32,62	27,64
17:0	Margaric acid	Saturated	0,70	0,62	0,49	0,61	0,66	0,53
16:0 2OH		Saturated	0,30	0,25	0,00			
18:0	Stearic acid	Saturated	9,95	8,68	7,87	14,52	16,51	9,23
19:0	Nonadecylic acid	Saturated	0,31	0,47	0,00			
20:0	Arachidic acid	Saturated	0,47	1,21	0,00			

	First ejaculate %	Fourth ejaculate %
Total Unsaturated	**53,01**	**44,65**
Total Saturated	**46,99**	**55,35**

Table S3. Total protein identified in in sperm extract from Nellore bulls at rest and during sexual activity. The proteins were identified using Peaks v.7 software.

Total proteins	
UniProt ID	**Description**
A0A077S1J5	Lysozyme A
A0A0F7RQ40	D-dopachrome tautomerase
A0A0K1LCB1	Piwi-like protein 1
A0A140T871	glutamate dehydrogenase [NAD
A0A140T8A5	Isocitrate dehydrogenase [NADP]
A0A1K0FUD3	Globin C1
A0A3Q1LFG5	Testis expressed 26
A0A3Q1LFK7	Piercer of microtubule wall 2 protein

A0A3Q1LGN5	electron-transferring-flavoprotein dehydrogenase
A0A3Q1LJB2	IF rod domain-containing protein
A0A3Q1LKA9	SERPIN domain-containing protein
A0A3Q1LLP1	Beta-defensin 109-like
A0A3Q1LMV9	Epiplakin 1
A0A3Q1LPL0	Dynein light chain roadblock
A0A3Q1LQK0	Cytochrome b5 domain containing 1
A0A3Q1LS74	**Complement factor H**
A0A3Q1LSI9	Calmodulin 2
A0A3Q1LXA8	**inorganic diphosphatase**
A0A3Q1LYL5	Propionyl-CoA carboxylase subunit alpha
A0A3Q1LZZ7	MDK
A0A3Q1M0L3	RNA helicase
A0A3Q1M1C3	COX6C domain-containing protein
A0A3Q1M1D0	Mitochondrial glutathione transporter SLC25A39
A0A3Q1M2W7	Dynein axonemal heavy chain 6
A0A3Q1M3K6	Leucine-rich repeat-containing protein 37B-like
A0A3Q1M4H9	Eppin-like
A0A3Q1M4K3	Ubiquitin-like domain-containing protein
A0A3Q1M4L0	HipN domain-containing protein
A0A3Q1M4T9	Outer dense fiber of sperm tails 3 like 2
A0A3Q1M5T5	Calcium/calmodulin dependent protein kinase IV
A0A3Q1M6C6	Calmodulin 1
A0A3Q1M7H2	Dynein axonemal heavy chain 17
A0A3Q1M8H0	Kazal-like domain-containing protein
A0A3Q1M9J8	Calcium-binding mitochondrial carrier protein SCaMC-1-like
A0A3Q1M9N4	AU RNA binding methylglutaconyl-CoA hydratase
A0A3Q1MA45	Hensin
A0A3Q1MB60	S100P-binding protein
A0A3Q1MBY2	MICOS complex subunit
A0A3Q1MDA5	Mesothelin
A0A3Q1MDT8	Glutamine amidotransferase class 1 domain containing 3
A0A3Q1ME83	Cilia and flagella associated protein 70
A0A3Q1MF13	Apolipoprotein A-I-binding protein
A0A3Q1MG14	Theg spermatid protein
A0A3Q1MGC0	propionate--CoA ligase
A0A3Q1MGG8	IQ motif containing N
A0A3Q1MI01	**Prosaposin**
A0A3Q1MI36	Protein kinase domain-containing protein
A0A3Q1MIM1	Binder of sperm protein homolog 1
A0A3Q1MKC8	**Keratin type II**
A0A3Q1MKK4	Prohibitin
A0A3Q1MKZ2	Acyl-CoA_dh_1 domain-containing protein

A0A3Q1MPL2	Chromosome 26 C10orf82 homolog
A0A3Q1MQK5	**Midkine**
A0A3Q1MQM3	ST13 Hsp70 interacting protein
A0A3Q1MUQ5	Solute carrier family 25 member 12
A0A3Q1MYU9	Sperm acrosome associated 9
A0A3Q1N023	CKLF like MARVEL transmembrane domain containing 1
A0A3Q1N0C4	Deleted in malignant brain tumors 1 protein
A0A3Q1N1A8	Deleted in malignant brain tumors 1 protein-like
A0A3Q1N1R0	EF-hand domain-containing family member C2
A0A3Q1N235	Dihydrolipoamide acetyltransferase component of pyruvate dehydrogenase complex
A0A3Q1N375	Multifunctional fusion protein
A0A3Q1N522	Ubiquitin carboxyl-terminal hydrolase
A0A3Q1N5Z4	Ig-like domain-containing protein
A0A3Q1N8V4	Lymphocyte antigen 6 family member K
A0A3Q1NEQ8	Beta-defensin 1
A0A3Q1NKS6	oxoglutarate dehydrogenase
A0A3Q1NLY8	Dynein light chain
A0A3Q1NMM9	Dynein axonemal heavy chain 12
A0A3Q8WRY0	**S100 calcium binding protein A9**
A0A3Q8WS74	S100 calcium binding protein A8
A0A3S5ZPC1	Synaptophysin like 1
A0A452DHZ5	**Nucleobindin-1**
A0A452DI02	palmitoyl-protein hydrolase
A0A452DIK0	NADH dehydrogenase 1 alpha subcomplex subunit 12
A0A452DIM7	Calmodulin 3
A0A452DIQ5	GLOBIN domain-containing protein
A0A452DIU2	cAMP-dependent protein kinase
A0A452DJG1	H-transporting two-sector ATPase
A0A4W2BP54	Jacalin-type lectin domain-containing protein
A0A5B8TVZ0	CEACAM32
A0A6P5C9R4	protein LEG1 homolog
A0A8E6LSW0	NADH:ubiquinone reductase
A0JN77	Triokinase/FMN cyclase
A0JNI4	Serine racemase
A0JNK3	Serine protease HTRA2, mitochondrial
A0JNM2	Thioredoxin
A0JNM6	Lysozyme-like protein 1
A0JNP2	Secretoglobin family 1D member
A1A4I8	Exportin 7
A1A4N9	Nucleoside diphosphate kinase
A1A4P8	Family with sequence similarity 209, member A
A1A4R1	Histone H2A type 2-C
A1L524	Septin 4

A1L5B1	Proteasome 26S non-ATPase subunit 7
A3KFF6	Postacrosomal sheath WW domain-binding protein
A3KMY8	Beta-glucuronidase
A4FV03	UBA6 protein
A4FV90	Propionyl-CoA carboxylase alpha chain, mitochondrial
A4IF87	Dihydroxyacetone phosphate acyltransferase
A4IFI4	PAOX protein
A4IFM8	Actin, alpha 1, skeletal muscle
A4IFP2	KRT4 protein
A5D7D1	Alpha-actinin-4
A5D7M6	KRT5 protein
A5D7N3	Transmembrane protein 11, mitochondrial
A5D7Q2	Igh protein
A5D7Q3	Septin-12
A5D7S5	SLC25A35 protein
A5D973	Alpha isoform of regulatory subunit A, protein phosphatase 2
A5D9D1	**Vanin 2**
A5D9E7	Mitochondrial trifunctional protein, beta subunit
A5D9G3	Succinate-CoA ligase subunit beta
A5PJD4	KLKBL4 protein
A5PJF7	C-C motif chemokine
A5PJL8	**C1QTNF5 protein**
A5PK42	Outer dynein arm-docking complex subunit 4
A5PK61	Histone H3.3C
A5PK65	D-dopachrome decarboxylase
A5PK67	MGC165862 protein
A5PK71	Parkin coregulated gene protein
A5PKG4	Cysteine desulfurase, mitochondrial
A5PKI3	Protein FAM3C
A5PKM0	glutathione transferase
A6H758	C11H9ORF9 protein
A6H768	Galactokinase
A6H782	Tektin-3
A6H798	LOC616153 protein
A6QLB8	[tau protein] kinase
A6QLG3	Protein-serine/threonine kinase
A6QLU1	Glycerol-3-phosphate dehydrogenase, mitochondrial
A6QNM9	SLC25A12 protein
A6QNW3	PIGR protein
A6QNX2	DPP7 protein
A6QNX5	Keratin, type II cytoskeletal 78
A6QNZ7	Keratin 10
A6QP39	**MSLN protein**

A6QPC0	Uncharacterized protein C10orf82 homolog
A6QPE3	TEX101 protein
A6QPH7	AKR7A2 protein
A6QPK0	SCGB2A2 protein
A6QPP7	ELA2 protein
A6QPT4	MPO protein
A6QPZ4	SERPINB4 protein
A6QQ65	LOC789612 protein
A6QQ77	Sperm acrosome membrane-associated protein 3
A6QQ83	THEM2 protein
A6QR35	Secretory carrier-associated membrane protein
A7E3B2	Deoxyribonuclease-1
A7E3P5	15-oxoprostaglandin 13-reductase
A7E3Q2	Heat shock 70kDa protein 1A
A7E3S8	Heat shock 70kD protein binding protein
A7E3V1	succinate dehydrogenase
A7E3W2	Galectin-3-binding protein
A7MAZ2	STX12 protein
A7MAZ5	Histone H1.3
A7MB90	non-specific serine/threonine protein kinase
A7MBA2	26S proteasome non-ATPase regulatory subunit 1
A7MBH5	Outer dynein arm-docking complex subunit 3
A7MBJ5	Cullin-associated NEDD8-dissociated protein 1
A7YWE4	Delta-1-pyrroline-5-carboxylate dehydrogenase, mitochondrial
A7YY24	IGBP1 protein
A7Z066	Calnexin
A8E4N3	Radial spoke head protein 3 homolog
A8E4P3	**STOM protein**
A8SMG2	Testis-expressed protein 43
B0JYN1	**Cathepsin L2**
B0JYN8	Proteasome subunit beta
B0JYQ0	**ALB protein**
C9QNT9	TEPP protein
D4QBB3	**Hemoglobin beta**
D4QBB4	Globin A1
E1B6Z6	Lipocalin 2
E1B715	Kinesin-like protein
E1B748	Hypoxia up-regulated 1
E1B7A4	GLIPR1 like 2
E1B7Q2	nucleoside-diphosphate kinase
E1B7S8	Acrosin-binding protein
E1B836	Enkurin
E1B8N5	Sodium/potassium-transporting ATPase subunit alpha

E1B8W3	Outer dynein arm-docking complex subunit 2
E1B993	Ankyrin repeat and EF-hand domain containing 1
E1B9F6	Elongation factor 1-alpha
E1B9H0	Beta-hexosaminidase
E1B9P4	Epididymal sperm binding protein 1
E1B9R5	Dynein axonemal heavy chain 8
E1B9Y3	Lipocalin 12
E1B9Z2	Leucine zipper and EF-hand containing transmembrane protein 2
E1BA36	Sperm associated antigen 17
E1BBK6	Nephronectin
E1BBM9	Disintegrin and metalloproteinase domain-containing protein 5-lik
E1BBT9	Heat shock protein family A
E1BC58	RAB2B, member RAS onco family
E1BCN4	**AMP-binding domain-containing protein**
E1BCN8	Phosphoethanolamine/phosphocholine phosphatase 1
E1BCP9	Galactosidase beta 1 like
E1BCR1	ATP binding cassette subfamily A member 3
E1BCW3	ATP-dependent 6-phosphofructokinase
E1BD64	Mitochondrial pyruvate carrier
E1BD83	Proteasome subunit alpha type
E1BDA8	Izumo sperm-egg fusion 1
E1BDM7	Zinc finger MYND-type containing 12
E1BDQ6	NME/NM23 family member 5
E1BE64	Testis specific 10
E1BED9	Glutathione S-transferase omega
E1BFG0	aldehyde dehydrogenase
E1BFM2	Serine protease 50
E1BH06	Complement component 4A
E1BHV9	Ornithine decarboxylase antizyme 3
E1BHW8	UBX domain protein 11
E1BI52	Serine protease 42
E1BI82	Inhibitor of carbonic anhydrase
E1BIE7	PGAM family member 5, mitochondrial serine/threonine protein phosphatase
E1BIN5	Cullin 3
E1BJC4	Piwi like RNA-mediated silencing 1
E1BJD3	Transmembrane protein 190
E1BJG2	Radial spoke head 6 homolog A
E1BJL8	Folate receptor alpha
E1BKF9	Cilia- and flagella-associated protein 52
E1BKH1	**EF-hand domain-containing protein 1**
E1BLG0	Adenylate kinase 8
E1BLI4	CUB domain-containing protein
E1BLK7	Mitochondria-eating protein

E1BLW6	Serine protease 55
E1BM25	Cilia and flagella associated protein 46
E1BM47	Maestro heat like repeat family member 2B
E1BM93	Retinol dehydrogenase 11
E1BMD1	Cilia- and flagella-associated protein 43
E1BMY1	NADH dehydrogenase 1 beta subcomplex subunit 4
E1BN01	Dynein axonemal light intermediate chain 1
E1BN79	Carboxylic ester hydrolase
E1BNL3	Zonadhesin
E1BNQ4	ATP-dependent
E1BNS9	L-lactate dehydrogenase
E1BP40	Cilia and flagella associated protein 61
E1BP91	Aminopeptidase
E1BPM9	Dynein axonemal intermediate chain 2
E2GEZ1	Mitochondrial import receptor subunit TOM22 homolog
E2GEZ2	Translocase of outer mitochondrial membrane 40A
F1MB08	phosphopyruvate hydratase
F1MB15	Fibrous sheath interacting protein 2
F1MB26	Ectonucleoside triphosphate diphosphohydrolase 1
F1MB32	Alpha-2-macroglobulin like 1
F1MBQ1	Serine/threonine-protein phosphatase with EF-hands
F1MBU8	Dpy-19 like 2
F1MBZ1	Kelch like family member 10
F1MC11	Keratin, type I cytoskeletal 14
F1MCF5	Glutathione peroxidase
F1MDK8	ADP/ATP translocase
F1ME38	Ubiquitin like modifier activating enzyme 6
F1MEM9	Tetratricopeptide repeat domain 19
F1MEY3	Testis anion transporter 1
F1MF48	Hydroxysteroid dehydrogenase-like protein 2
F1MF73	Chromosome 3 C1orf56 homolog
F1MFA3	Presequence protease, mitochondrial
F1MFB3	Gem-associated protein 6
F1MGQ1	Deoxyribonuclease
F1MGU7	Fibrinogen gamma-B chain
F1MHK9	ATP-binding cassette sub-family A member 3-like
F1MI34	Cilia and flagella associated protein 65
F1MIC9	Dynactin subunit 1
F1MIH9	Phospholipase B-like
F1MIM1	Prostate and testis expressed 2
F1MJQ7	Fibronectin type III domain-containing protein 8
F1MJY8	Interferon-gamma-inducible GTPase IFGGE protein
F1MK55	Dynein axonemal heavy chain 2

F1MKF8	Sulfide quinone oxidoreductase
F1MKL5	ADAM metallopeptidase domain 3A
F1MKR7	Cilia and flagella associated protein 77
F1MKX4	Proteasome activator complex subunit 4
F1MLB8	ATP synthase subunit alpha
F1MLS4	Membrane spanning 4-domains A14
F1MLW2	**BPI fold-containing family B member 1**
F1MLX0	Fumarylacetoacetate hydrolase domain containing 2A
F1MM32	Sulfhydryl oxidase
F1MMM6	Slit guidance ligand 3
F1MMP2	Cilia and flagella associated protein 57
F1MMV1	EF-hand domain-containing family member B
F1MMY0	SSD domain-containing protein
F1MMZ2	Ferritin
F1MN04	SAICAR synthetase
F1MN78	Serpin B4
F1MNH2	Radial spoke head component 1
F1MNH9	WAP four-disulfide core domain protein 13
F1MNL6	Nucleoporin 210 like
F1MNT1	Nucleoporin 155
F1MNT3	Hormone-sensitive lipase
F1MP86	Tetraspanin
F1MPE5	Importin 5
F1MPF5	Chromosome 7 open reading frame 61
F1MPR3	Calcium-transporting ATPase
F1MPU0	Clathrin heavy chain
F1MQ37	Myosin heavy chain 9
F1MQX0	Acetyl-coenzyme A synthetase
F1MR35	Angiotensin-converting enzyme
F1MRU4	Dynein axonemal heavy chain 3
F1MS23	**Lipocln_cytosolic_FA-bd_dom domain-containing protein**
F1MSC3	acetyl-CoA carboxylase
F1MSL8	IQ motif and ubiquitin domain containing
F1MSP8	Dynein axonemal heavy chain 10
F1MSZ0	Serine/threonine kinase like domain containing 1
F1MT40	RAN binding protein 17
F1MTN9	NME/NM23 family member 8
F1MTR1	IQ motif containing GTPase activating protein 2
F1MTY9	heme oxygenase
F1MUB8	Spermatosis and centriole associated 1
F1MUF4	**Beta-galactosidase**
F1MUP9	Vesicle amine transport 1
F1MUV1	fatty acid amide hydrolase

F1MUZ9	60 kDa heat shock protein, mitochondrial
F1MVB5	Chromosome 23 C6orf136 homolog
F1MVK1	Complement C4 gamma chain
F1MVL0	IQ motif containing with AAA domain 1 like
F1MVX2	Glutathione S-transferase LANCL1
F1MW14	Ran guanine nucleotide release factor
F1MWD3	T-complex protein 1 subunit epsilon
F1MWF0	Huntingtin interacting protein 1
F1MWN8	Cilia and flagella associated protein 58
F1MWR3	Electron transfer flavoprotein subunit alpha
F1MWT0	alpha-mannosidase
F1MWY9	Enoyl-CoA delta isomerase 2
F1MX07	Tektin
F1MX39	RAB42, member RAS oncogene family
F1MX68	Carboxypeptidase
F1MX88	Solute carrier family 25 member 13
F1MXP7	VWFA domain-containing protein
F1MXQ5	Calpain 11
F1MXX0	MICOS complex subunit MIC60
F1MY02	Disintegrin and metalloproteinase domain-containing protein 1a-like
F1MY12	NTR domain-containing protein
F1MY24	Chaperonin containing TCP1 subunit 8 like 2
F1MY28	Large proline-rich protein BAG6
F1MY93	Leucine rich repeat containing 34
F1MYA6	IZUMO family member 4
F1MYH5	A-kinase anchoring protein 4
F1MZB5	Testis-expressed sequence 37 protein
F1MZC0	Aldo-keto reductase family 7 member A2
F1MZJ1	Tektin bundle-interacting protein 1
F1MZU2	Vesicle-fusing ATPase
F1N058	Ropporin-1
F1N0A4	Acyl-CoA dehydrogenase family member 9
F1N0E5	T-complex protein 1 subunit delta
F1N0M0	Tripeptidyl-peptidase 2
F1N0T8	Synaptogyrin
F1N152	Serine protease HTRA1
F1N191	Interleukin 4 induced 1
F1N1S0	Single-stranded DNA-binding protein
F1N206	Dihydrolipoyl dehydrogenase
F1N2C7	AarF domain containing kinase 5
F1N2F2	Phosphoglycerate mutase
F1N2N9	Outer dynein arm-docking complex subunit 1
F1N2S7	Testis specific serine kinase 6

F1N343	Coiled-coil domain containing 136
F1N369	Zona pellucida binding protein
F1N3F1	LETM1 domain-containing protein 1
F1N3G6	Phospholipid-transporting ATPase
F1N430	**Metalloproteinase inhibitor 2**
F1N450	Regulator of G protein signaling 22
F1N4A1	Armadillo repeat containing 12
F1N556	Ubiquitin carboxyl-terminal hydrolase 7
F1N594	Radial spoke head 14 homolog
F1N5R7	Dynein axonemal heavy chain 7
F1N650	**Annexin**
F1N690	Acetyltransferase component of pyruvate dehydrogenase complex
F1N6K8	Uncharacterized protein
F1N6M5	Coiled-coil domain containing 183
F1N6Q0	DnaJ heat shock protein family
F1N6T4	NME/NM23 nucleoside diphosphate kinase 4
F1N7D7	Dystroglycan 1
F1N7P3	Lysophosphatidylcholine acyltransferase 2B
F1N7X7	Golgi associated RAB2B interactor family member 3
F2Z4F0	Actin related protein 1A
F2Z4F5	Dipeptidyl peptidase 3
F6PRB5	Enoyl-CoA hydratase 1
F6PXW3	Actin related protein T3
F6QGE6	Acyl-CoA thioesterase 13
F6QJG7	Zona pellucida binding protein 2
F6QQ46	Chromosome 10 C15orf48 homolog
F6R6Q1	FAD synthase
F6RGR9	Leucine zipper protein 2
F6RLA2	Testis specific serine kinase 4
F6RP72	Tubulin alpha chain
G1K1H0	Disintegrin and metalloproteinase domain-containing protein 2
G3MWG4	isoleucine--tRNA ligase
G3MWP1	Elastase, neutrophil expressed
G3MWV5	H1.4 linker histone, cluster member
G3MX69	LRRC37AB_C domain-containing protein
G3MXB5	IgA constant region
G3MY97	DUF3699 domain-containing protein
G3MYD7	Histone H3
G3MZ95	Four and a half LIM domains 1
G3MZM7	Protein phosphatase inhibitor 2
G3MZM8	vitamin-K-epoxide reductase
G3MZT7	Disintegrin and metalloproteinase domain-containing protein 30-like
G3MZZ6	Protein-L-isoaspartate O-methyltransferase

G3N0F4	Peptidase S1 domain-containing protein
G3N0F7	Testis expressed 50
G3N0H2	Chromosome 11 C2orf16 homolog
G3N0V2	Keratin, type II cytoskeletal 1
G3N136	Testis specific serine kinase 2
G3N1C8	Dynein axonemal heavy chain 1
G3N1S7	Cilia and flagella associated protein 100
G3N284	Actin related protein T1
G3N2H4	Azurocidin 1
G3N2P2	Histone domain-containing protein
G3N3N1	ADP-ribosylation factor 6
G3X6E2	Family with sequence similarity 166 member A
G3X6J2	FAM75 domain-containing protein
G3X6L8	Nipsnap homolog 3A
G3X6U1	Aldehyde dehydrogenase 1 family member A2
G3X7X2	Solute carrier family 25 member 32
G3X800	Disintegrin and metalloproteinase domain-containing protein 20-like
G3X8C3	Serpin family B member 4
G3X8E3	Beta-microseminoprotein
G5E519	Coiled-coil domain-containing protein 39
G5E521	NAD-dependent protein deacetylase
G5E531	T-complex protein 1 subunit alpha
G5E5A3	EF-hand domain-containing protein
G5E5T5	Immunoglobulin heavy constant mu
G5E622	ADAM metallopeptidase domain 20
G5E6C5	ADAM9 protein
G8CY17	Beta-defensin
G8JKV7	procollagen-lysine 5-dioxygenase
I6NUJ4	Choline transporter-like protein
M5FJY9	Phosphoglycolate phosphatase
M5FK65	Protease, serine, 21-like
O02691	3-hydroxyacyl-CoA dehydrogenase type-2
O46414	Ferritin heavy chain
O46415	Ferritin light chain
O46563	V-type proton ATPase subunit H
O46629	Trifunctional enzyme subunit beta, mitochondrial
O62768	Thioredoxin reductase 1, cytoplasmic
O77588	Procollagen-lysine,2-oxoglutarate 5-dioxygenase 1
O77779	Fertilin alpha
O77784	Isocitrate dehydrogenase [NAD] subunit beta, mitochondrial
O77797	A-kinase anchor protein 3
O77834	Peroxiredoxin-6
O97650	Succinate dehydrogenase Ip subunit

O97725	NADH dehydrogenase 1 alpha subcomplex subunit 12
O97764	Zeta-crystallin
P00125	Cytochrome c1, heme protein, mitochondrial
P00126	Cytochrome b-c1 complex subunit 6, mitochondrial
P00129	Cytochrome b-c1 complex subunit 7
P00130	Cytochrome b-c1 complex subunit 9
P00366	Glutamate dehydrogenase 1, mitochondrial
P00423	Cytochrome c oxidase subunit 4 isoform 1, mitochondrial
P00426	Cytochrome c oxidase subunit 5A, mitochondrial
P00428	Cytochrome c oxidase subunit 5B, mitochondrial
P00442	Superoxide dismutase [Cu-Zn]
P00514	cAMP-dependent protein kinase type I-alpha regulatory subunit
P00515	cAMP-dependent protein kinase type II-alpha regulatory subunit
P00517	cAMP-dependent protein kinase catalytic subunit alpha
P00570	Adenylate kinase isoenzyme 1
P00669	Seminal ribonuclease
P00727	Cytosol aminopeptidase
P00829	ATP synthase subunit beta, mitochondrial
P00921	Carbonic anhydrase 2
P01966	**Hemoglobin subunit alpha**
P02070	Hemoglobin subunit beta
P02253	Histone H1.2
P02722	ADP/ATP translocase 1
P02784	Seminal plasma protein PDC-109
P04038	Cytochrome c oxidase subunit 6C
P04272	Annexin A2
P04394	NADH dehydrogenase flavoprotein 2
P04557	Seminal plasma protein A3
P05307	Protein disulfide-isomerase
P05630	ATP synthase subunit delta, mitochondrial
P05631	ATP synthase subunit gamma, mitochondrial
P06394	Keratin, type I cytoskeletal 10
P06833	Caltrin
P08728	Keratin, type I cytoskeletal 19
P08760	GTP:AMP phosphotransferase AK3, mitochondrial
P0C0S9	Histone H2A type 1
P0CB32	Heat shock 70 kDa protein 1-like
P0CG53	Polyubiquitin-B [Cleaved into: Ubiquitin]
P0CH28	Polyubiquitin-C [Cleaved into: Ubiquitin-related; Ubiquitin]
P10096	Glyceraldehyde-3-phosphate dehydrogenase
P10152	Angiogenin-1
P11024	NADP transhydrogenase

P11179	Dihydrolipoyllysine-residue succinyltransferase component of 2-oxoglutarate dehydrogenase complex
P11966	Pyruvate dehydrogenase E1 component subunit beta, mitochondrial
P12234	Phosphate carrier protein, mitochondrial
P12344	Aspartate aminotransferase, mitochondrial
P13135	Calpain small subunit 1
P13184	Cytochrome c oxidase subunit 7A2, mitochondrial
P13271	Cytochrome b-c1 complex subunit 8
P13272	Cytochrome b-c1 complex subunit Rieske, mitochondrial
P13600	Beta-nerve growth factor
P13619	ATP synthase F
P13621	ATP synthase subunit O, mitochondrial
P13696	Phosphatidylethanolamine-binding protein 1
P15103	Glutamine synthetase
P15246	Protein-L-isoaspartate
P15690	NADH-ubiquinone oxidoreductase 75 kDa subunit, mitochondrial
P16116	Aldo-keto reductase family 1 member B1
P17248	Tryptophan--tRNA ligase, cytoplasmic
P17453	Bactericidal permeability-increasing protein
P17694	NADH dehydrogenase iron-sulfur protein 2
P17697	**Clusterin**
P19858	L-lactate dehydrogenase A chain
P20000	Aldehyde dehydrogenase, mitochondrial
P20004	Aconitate hydratase, mitochondrial
P20427	Casein kinase II subunit alpha'
P21856	Rab GDP dissociation inhibitor alpha
P22226	**Cathelicidin-1**
P22292	Mitochondrial 2-oxoglutarate/malate carrier protein
P22439	Pyruvate dehydrogenase protein X component
P23004	Cytochrome b-c1 complex subunit 2, mitochondrial
P23356	Ubiquitin carboxyl-terminal hydrolase isozyme L1
P23709	NADH dehydrogenase iron-sulfur protein 3
P23934	NADH dehydrogenase iron-sulfur protein 6
P23935	NADH dehydrogenase 1 alpha subcomplex subunit 5
P24627	Lactotransferrin
P25326	Cathepsin S
P25708	NADH dehydrogenase flavoprotein 1
P25975	Procathepsin L
P28291	C-C motif chemokine 2
P28782	**Protein S100-A8**
P29392	**Spermadhesin-1**
P31039	Succinate dehydrogenase flavoprotein subunit
P31096	Osteopontin

P31404	V-type proton ATPase catalytic subunit A
P31408	V-type proton ATPase subunit B, brain isoform
P31800	Cytochrome b-c1 complex subunit 1, mitochondrial
P31976	**Ezrin**
P32007	ADP/ATP translocase 3
P33097	Aspartate aminotransferase, cytoplasmic
P33672	Proteasome subunit beta type-3
P34942	NADH dehydrogenase 1 alpha subcomplex subunit 10
P34943	NADH dehydrogenase 1 alpha subcomplex subunit 9
P35662	Cylicin-1
P35720	Succinate dehydrogenase cytochrome b560 subunit, mitochondrial
P37141	Glutathione peroxidase 3
P38657	Protein disulfide-isomerase A3
P41976	Superoxide dismutase [Mn], mitochondrial
P42026	NADH dehydrogenase iron-sulfur protein 7
P42028	NADH dehydrogenase iron-sulfur protein 8
P42029	NADH dehydrogenase 1 alpha subcomplex subunit 8
P45478	Palmitoyl-protein thioesterase 1
P45879	Voltage-dependent anion-selective channel protein 1
P46160	Beta-defensin 2
P46161	Beta-defensin 3
P46168	Beta-defensin 10
P46193	Annexin A1
P48818	Very long-chain specific acyl-CoA dehydrogenase, mitochondrial
P49951	Clathrin heavy chain 1
P50397	Rab GDP dissociation inhibitor beta
P52174	Nucleoside diphosphate kinase A 1
P52175	Nucleoside diphosphate kinase A 2
P52193	Calreticulin
P54281	Calcium-activated chloride channel regulator 1
P55206	C-type natriuretic peptide
P56701	26S proteasome non-ATPase regulatory subunit 2
P58352	Solute carrier family 2, facilitated glucose transporter member 3
P60712	Actin, cytoplasmic 1
P61585	Transforming protein RhoA
P61603	10 kDa heat shock protein, mitochondrial
P62157	Calmodulin
P62194	26S proteasome regulatory subunit 8
P62261	14-3-3 protein epsilon
P62739	Actin, aortic smooth muscle
P62803	Histone H4
P62808	Histone H2B type 1
P62894	Cytochrome c

P62992	Ubiquitin-40S ribosomal protein S27a
P63026	Vesicle-associated membrane protein 2
P63048	Ubiquitin-60S ribosomal protein L40
P63103	14-3-3 protein zeta/delta
P63171	Dynein light chain Tctex-type 1
P63258	Actin, cytoplasmic 2
P67774	Serine/threonine-protein phosphatase 2A catalytic subunit alpha isoform
P67810	Signal peptidase complex catalytic subunit SEC11A
P67827	Casein kinase I isoform alpha
P67868	Casein kinase II subunit beta
P68002	Voltage-dependent anion-selective channel protein 2
P68103	Elongation factor 1-alpha 1
P68138	Actin, alpha skeletal muscle
P68432	Histone H3.1
P68530	Cytochrome c oxidase subunit 2
P69678	Protein CutA
P79110	Tricarboxylate transport protein, mitochondrial
P79136	F-actin-capping protein subunit beta
P79343	Acrosin
P79345	NPC intracellular cholesterol transporter 2
P80025	Lactoperoxidase
P80177	Macrophage migration inhibitory factor
P80311	Peptidyl-prolyl cis-trans isomerase B
P81019	Seminal plasma protein BSP-30 kDa
P81134	Renin receptor
P81187	**Complement factor B**
P81265	Polymeric immunoglobulin receptor
P82908	Alpha-ketoglutarate dehydrogenase component 4
P84080	ADP-ribosylation factor 1
P84081	ADP-ribosylation factor 2
P84227	Histone H3.2
Q00361	ATP synthase subunit e, mitochondrial
Q02337	D-beta-hydroxybutyrate dehydrogenase, mitochondrial
Q02368	NADH dehydrogenase 1 beta subcomplex subunit 7
Q02369	NADH dehydrogenase 1 beta subcomplex subunit 9
Q02370	NADH dehydrogenase 1 alpha subcomplex subunit 2
Q02372	NADH dehydrogenase 1 beta subcomplex subunit 8
Q02373	NADH dehydrogenase 1 beta subcomplex subunit 10
Q02827	NADH dehydrogenase 1 subunit C2
Q04467	Isocitrate dehydrogenase [NADP], mitochondrial
Q05752	NADH dehydrogenase 1 alpha subcomplex subunit 7
Q07130	UTP--glucose-1-phosphate uridylyltransferase
Q08DC0	Serpin peptidase inhibitor, clade E

Q08DD1	Arylsulfatase A
Q08DK4	Mitochondrial glutamate carrier 1
Q08DM3	Malic enzyme
Q08DN5	Carnitine O-acetyltransferase
Q08DW2	Phosphoribosyl pyrophosphate synthase-associated protein 1
Q0II87	Transcription factor A, mitochondrial
Q0IIC1	Acyl-CoA synthetase bubblegum family member 2
Q0IID8	1-acylglycerol-3-phosphate O-acyltransferase 5
Q0IIG5	ATP-dependent 6-phosphofructokinase, muscle type
Q0P565	5'-deoxynucleotidase HDDC2
Q0V8B6	Tripeptidyl-peptidase 1
Q0VC58	Trimeric intracellular cation channel type B
Q0VCA3	Mitochondrial proton/calcium exchanger protein
Q0VCH6	Probable mitochondrial glutathione transporter SLC25A40
Q0VCU3	Cathepsin F
Q0VCX2	Endoplasmic reticulum chaperone BiP
Q0VCY1	Vesicle-associated membrane protein-associated protein A
Q148D3	Fumarate hydratase, mitochondrial
Q148G2	Glucose-6-phosphatase 3
Q148H0	MICOS complex subunit MIC26
Q148I4	Acyl-CoA thioesterase 7
Q148N0	2-oxoglutarate dehydrogenase complex component E1
Q148N3	Matrix metallopeptidase 7
Q17QH8	Epimerase family protein SDR39U1
Q17QH9	Dynein regulatory complex protein 10
Q17QI3	Acetyl-CoA acetyltransferase 2
Q17QK3	Carboxypeptidase Q
Q17QL7	KRT15 protein
Q1JP95	Proteasome 26S ATPase subunit 3
Q1JPF2	NADH dehydrogenase
Q1LZB5	Mitochondrial import receptor subunit TOM40 homolog
Q1RML2	1-phosphatidylinositol 4,5-bisphosphate phosphodiesterase zeta-1
Q1RMN5	Spermatogenesis associated 3
Q1RMN8	Immunoglobulin light chain, lambda gene cluster
Q1RMP3	CutA divalent cation tolerance homolog
Q1RMP7	Probable inactive peptidyl-prolyl cis-trans isomerase-like 6
Q1RMX2	Ubiquitin-conjugating enzyme E2 D2
Q1RMX7	N-acetylneuraminate synthase
Q24JZ7	Succinyl-CoA:3-ketoacid-coenzyme A transferase
Q28017	Platelet-activating factor acetylhydrolase
Q28068	Calicin
Q28092	Cylicin-2
Q28120	Glutaminyl-peptide cyclotransferase

Q28851	ATP synthase subunit f, mitochondrial
Q28910	Mucin
Q29438	Outer dense fiber protein 1
Q29443	Serotransferrin
Q29444	Beta-mannosidase
Q29RK1	Citrate synthase, mitochondrial
Q29RK2	Pyruvate carboxylase, mitochondrial
Q29RM1	Mitochondrial thiamine pyrophosphate carrier
Q29RT3	MS4A13 protein
Q29RU5	Rhabdoid tumor deletion region gene 1
Q29RZ0	Acetyl-CoA acetyltransferase, mitochondrial
Q29S21	Keratin, type II cytoskeletal 7
Q2HJ55	Sorting and assembly machinery component 50 homolog
Q2HJ58	Ribose-phosphate pyrophosphokinase 1
Q2HJ97	Prohibitin-2
Q2HJB8	Tubulin alpha-8 chain
Q2HJD7	3-hydroxyisobutyrate dehydrogenase, mitochondrial
Q2HJF0	Serotransferrin-like
Q2HJH1	Aspartyl aminopeptidase
Q2HJH2	Ras-related protein Rab-1B
Q2KI07	ADP-ribosylation factor-like protein 8B
Q2KI42	26S proteasome non-ATPase regulatory subunit 11
Q2KIB0	Fumarylacetoacetate hydrolase domain-containing protein 2
Q2KIC7	**Serine/threonine-protein phosphatase**
Q2KID4	Dynein axonemal light chain 1
Q2KIG0	Electron transfer flavoprotein-ubiquinone oxidoreductase, mitochondrial
Q2KIK5	LOC767871 protein
Q2KIM0	**Tissue alpha-L-fucosidase**
Q2KIN2	Deoxyguanosine kinase
Q2KIS9	Tetraspanin-8
Q2KIU7	Radial spoke head protein 9 homolog
Q2KIV8	Glutathione S-transferase
Q2KIY5	Putative phospholipase B-like 2
Q2KJ44	Serine/threonine-protein phosphatase 2A activator
Q2KJ46	26S proteasome non-ATPase regulatory subunit 3
Q2KJ77	HSPA
Q2KJ81	AP-1 complex subunit mu-1
Q2KJB1	Septin-10
Q2KJC5	Hydroxyacyl-Coenzyme A dehydrogenase
Q2KJC9	Alpha-aminoadipic semialdehyde dehydrogenase
Q2KJD0	Tubulin beta-5 chain
Q2KJD2	Vesicle-associated membrane protein 3
Q2KJE5	Glyceraldehyde-3-phosphate dehydrogenase, testis-specific

Q2KJH9	4-trimethylaminobutyraldehyde dehydrogenase
Q2KJI7	AFG3-like protein 2
Q2M2T1	Histone H2B type 1-K
Q2M2U1	CYLC2 protein
Q2NKS5	Chromosome 22 C3orf84 homolog
Q2NKS8	peptidylprolyl isomerase
Q2NKT6	Uncharacterized protein MGC137036
Q2NKV1	Angiogenin, ribonuclease, RNase A family, 5
Q2NKZ1	T-complex protein 1 subunit eta
Q2NKZ3	ADAM metallopeptidase domain 32
Q2NKZ8	glycerol kinase
Q2NL10	Syntaxin binding protein 2
Q2NL21	DnaJ homolog subfamily C member 11
Q2NL29	Inositol-3-phosphate synthase 1
Q2T9M4	Dynein regulatory complex subunit 7
Q2T9N0	Fibrous sheath CABYR-binding protein
Q2T9N7	Lysozyme-like protein 4
Q2T9Q6	Tektin-2
Q2T9R6	Omega-amidase NIT2
Q2T9S4	Glycerol-3-phosphate phosphatase
Q2T9T0	Protein phosphatase 1 regulatory subunit 32
Q2T9U2	Outer dense fiber protein 2
Q2T9W3	Coiled-coil domain-containing protein 63
Q2T9W4	Actin-like protein 9
Q2T9X2	T-complex protein 1 subunit delta
Q2T9X5	Sperm acrosome developmental regulator
Q2T9X9	Armadillo repeat containing 3
Q2T9Y3	Pyruvate dehydrogenase E1 component subunit alpha
Q2TA11	Cilia- and flagella-associated protein 107
Q2TA14	Lysosomal Pro-X carboxypeptidase
Q2TA16	Dynein regulatory complex subunit 2
Q2TA22	Long-chain-fatty-acid--CoA ligase
Q2TA28	Signal-regulatory protein delta
Q2TA38	Tektin-4
Q2TA43	Actin-related protein T2
Q2TBG5	Non-metastatic cells 4, protein expressed in
Q2TBG8	Ubiquitin carboxyl-terminal hydrolase isozyme L3
Q2TBH0	Outer dense fiber protein 3
Q2TBH3	Actin related protein M1
Q2TBI4	Heat shock protein 75 kDa, mitochondrial
Q2TBP7	c-Myc-binding protein
Q2TBQ6	Heat shock protein beta-9
Q2TBR0	Propionyl-CoA carboxylase beta chain, mitochondrial

Q2TBR1	5'-nucleotidase, cytosolic IB
Q2TBS5	Serine peptidase inhibitor, Kazal type 2
Q2TBV3	Electron transfer flavoprotein subunit beta
Q2TBW4	Polycystic kidney disease 2-like 2
Q2UVX4	**Complement C3**
Q2YDD6	Synaptogyrin-4
Q2YDD9	ADP/ATP translocase 4
Q2YDE4	Proteasome subunit alpha type-6
Q2YDE8	Golgi-associated RAB2 interactor protein 2
Q2YDG7	Sperm acrosome membrane-associated protein 1
Q2YDI7	Tektin-5
Q2YDI9	Ferritin, mitochondrial
Q2YDK3	Hyaluronidase
Q2YDK7	Thioredoxin domain containing 3
Q2YDL8	Uncharacterized protein LOC780846
Q2YDN4	Coiled-coil domain-containing protein 105
Q2YDN8	**Inactive serine/threonine-protein kinase VRK3**
Q32KL2	Proteasome subunit beta type-5
Q32KL7	Sperm equatorial segment protein 1
Q32KN6	Phosphoglycerate kinase
Q32KN8	Tubulin alpha-3 chain
Q32KP0	Spermatid-specific manchette-related protein 1
Q32KP2	Leucine-rich repeat-containing protein 23
Q32KP4	Abhydrolase domain containing 16B
Q32KR1	EF-hand calcium binding domain 6
Q32KR2	Acrosomal vesicle protein 1
Q32KR7	Hypothetical LOC539526
Q32KS2	Dynein axonemal intermediate chain 1
Q32KS3	F-actin-capping protein subunit alpha
Q32KT5	Uncharacterized protein C6orf136 homolog
Q32KU2	Probable inactive serine protease 37
Q32KU4	IQ domain-containing protein F5
Q32KV0	Phosphoglycerate mutase 2
Q32KX0	Isochorismatase domain-containing protein 2
Q32KY1	Dynein regulatory complex protein 1
Q32KZ2	Actin-like protein 7A
Q32KZ9	Tektin-1
Q32L04	Late cornified envelope-like proline-rich protein 1
Q32L54	Sperm associated antigen 6
Q32L61	Calcium binding tyrosine phosphorylation regulated
Q32L74	Aquaporin 7
Q32L77	Cilia- and flagella-associated protein 95
Q32L86	Transmembrane protein 126A

Q32L91	Actin-like protein 7B
Q32L99	Prostaglandin reductase 2
Q32LB5	GLIPR1-like protein 1
Q32LB7	V-type proton ATPase subunit E 2
Q32LD3	Ly6/PLAUR domain-containing protein 4
Q32LE0	Fascin actin-bundling protein 3
Q32LE5	Isoaspartyl peptidase/L-asparaginase
Q32LF7	Beta-1,4-galactosyltransferase
Q32LG3	Malate dehydrogenase, mitochondrial
Q32LG7	RING-type E3 ubiquitin transferase
Q32LH4	Deaminated glutathione amidase
Q32LI4	CSNK1A1 protein
Q32LJ7	RIB43A-like with coiled-coils protein 2
Q32LM0	Endophilin-B1
Q32LM2	Small glutamine-rich tetratricopeptide repeat-containing protein alpha
Q32LN4	Cilia- and flagella-associated protein 45
Q32LN6	Protein FAM205C
Q32LP8	Cysteine-rich secretory protein 2
Q32P61	Histone H2A
Q32P85	Dynein light chain roadblock-type 2
Q32P93	Glycosylphosphatidylinositol anchored molecule like
Q32PA1	CD59 glycoprotein
Q32PB1	Profilin-3
Q32PF2	ATP-citrate synthase
Q32PI5	Serine/threonine-protein phosphatase 2A 65 kDa regulatory subunit A alpha isoform
Q32S29	Histone H2B
Q3B7M2	Hydroxyacylglutathione hydrolase, mitochondrial
Q3B7N2	Alpha-actinin-1
Q3MHJ6	Acyl-Coenzyme A dehydrogenase family, member 9
Q3MHL4	Adenosylhomocysteinase
Q3MHL7	T-complex protein 1 subunit zeta
Q3MHM5	Tubulin beta-4B chain
Q3MHN0	Proteasome subunit beta type-6
Q3MHP2	Ras-related protein Rab-11B
Q3MHR0	Acyl-protein thioesterase 1
Q3MHR3	Dynein light chain 2, cytoplasmic
Q3MHW4	SQRDL protein
Q3MHW9	NADH-cytochrome b5 reductase 1
Q3MHX0	sulfite oxidase
Q3MHX5	Succinate--CoA ligase [GDP-forming] subunit beta, mitochondrial
Q3MHY9	ACTR1A protein
Q3SWW9	Serine/threonine-protein phosphatase PP1-beta catalytic subunit
Q3SWX2	Acyl-coenzyme A thioesterase 9, mitochondrial

Q3SYS3	Sperm surface protein Sp17
Q3SYS7	IQ domain-containing protein F1
Q3SYU2	Elongation factor 2
Q3SZ54	Eukaryotic initiation factor 4A-I
Q3SZ65	Eukaryotic initiation factor 4A-II
Q3SZ81	PSMC3 protein
Q3SZA4	Solute carrier family 25
Q3SZB4	Medium-chain specific acyl-CoA dehydrogenase, mitochondrial
Q3SZB7	Fructose-1,6-bisphosphatase 1
Q3SZI0	Mannose-6-phosphate isomerase
Q3SZI2	Lamin A/C
Q3SZK3	Growth hormone inducible transmembrane protein
Q3SZQ1	Nicastrin
Q3SZQ3	Spermatogenesis-associated protein 19, mitochondrial
Q3SZR5	Protein FAM166C
Q3SZT6	Protein Flattop
Q3SZT9	Cytochrome c 2
Q3SZV3	Elongation factor 1-gamma
Q3SZW1	Testis-specific serine/threonine-protein kinase 1
Q3SZW9	DnaJ
Q3SZX9	Coiled-coil domain-containing protein 113
Q3SZZ9	FGG protein
Q3T008	Septin
Q3T010	Phosphatidylethanolamine-binding protein 4
Q3T024	Ropporin-1-like protein
Q3T056	L-lactate dehydrogenase A-like 6B
Q3T067	Saccharopine dehydrogenase-like oxidoreductase
Q3T077	Tubulin polymerization-promoting protein family member 2
Q3T0B2	26S proteasome non-ATPase regulatory subunit 6
Q3T0C6	Sodium/potassium-transporting ATPase subunit beta-3
Q3T0C9	Synaptojanin-2-binding protein
Q3T0K2	T-complex protein 1 subunit gamma
Q3T0K7	MFGE8 protein
Q3T0P6	Phosphoglycerate kinase 1
Q3T0Q4	Nucleoside diphosphate kinase B
Q3T0R4	Dehydrogenase/reductase SDR family member 7B
Q3T0R7	3-ketoacyl-CoA thiolase, mitochondrial
Q3T0T0	Glycerophosphodiester phosphodiesterase 1
Q3T0U3	Es1 protein
Q3T0W4	Protein phosphatase 1 regulatory subunit 7
Q3T0X5	Proteasome subunit alpha type-1
Q3T0Y5	Proteasome subunit alpha type-2
Q3T0Z0	WAP four-disulfide core domain 2

Q3T114	2-iminobutanoate/2-iminopropanoate deaminase
Q3T145	Malate dehydrogenase, cytoplasmic
Q3T149	Heat shock protein beta-1
Q3T165	Prohibitin 1
Q3T172	ECH1 protein
Q3T186	Ribose-5-phosphate isomerase
Q3T189	Succinate dehydrogenase iron-sulfur subunit
Q3ZBD0	26S proteasome non-ATPase regulatory subunit 7
Q3ZBD7	Glucose-6-phosphate isomerase
Q3ZBF6	Short-chain specific acyl-CoA dehydrogenase, mitochondrial
Q3ZBG1	Ras-related protein Rab-14
Q3ZBH0	T-complex protein 1 subunit beta
Q3ZBT1	Transitional endoplasmic reticulum ATPase
Q3ZBV9	Dehydrogenase/reductase SDR family member 11
Q3ZBX9	Histone H2A.J
Q3ZBY4	Fructose-bisphosphate aldolase
Q3ZC07	Actin, alpha cardiac muscle 1
Q3ZC64	**Ephrin-A1**
Q3ZC87	Pyruvate kinase
Q3ZCF0	Dynactin subunit 2
Q3ZCF7	Ubiquitin-conjugating enzyme E2 D3
Q3ZCH0	Stress-70 protein, mitochondrial
Q3ZCH9	Haloacid dehalogenase-like hydrolase domain-containing protein 2
Q3ZCI4	6-phosphogluconate dehydrogenase, decarboxylating
Q3ZCI9	T-complex protein 1 subunit theta
Q3ZCK2	small monomeric GTPase
Q3ZCK9	Proteasome subunit alpha type-4
Q4GZT4	Broad substrate specificity ATP-binding cassette transporter ABCG
Q58CP0	Isocitrate dehydrogenase [NAD] subunit gamma, mitochondrial
Q58CS4	Seryl-tRNA synthetase 2
Q58D31	Sorbitol dehydrogenase
Q58D33	MYG1 protein
Q58D49	Corrinoid adenosyltransferase MMAB
Q58DG1	MYG1 exonuclease
Q58DJ4	serine--tRNA ligase
Q58DK1	Carnitine O-palmitoyltransferase 1, muscle isoform
Q58DM0	Isocitrate dehydrogenase [NAD] subunit, mitochondrial
Q58DM8	Enoyl-CoA hydratase, mitochondrial
Q58DP6	**Ribonuclease 4**
Q58DP7	Heat shock 27kDa protein 1
Q58DR8	Succinate--CoA ligase subunit alpha
Q58DS3	Solute carrier family 25 member 35
Q58DU5	Proteasome subunit alpha type-3

Q59HJ6	Lon protease homolog, mitochondrial
Q5DPW9	**Cystatin E/M**
Q5E946	Parkinson disease protein 7 homolog
Q5E956	Triosephosphate isomerase
Q5E987	Proteasome subunit alpha type-5
Q5E9B5	Actin, gamma-enteric smooth muscle
Q5E9D3	MICOS complex subunit MIC19
Q5E9F8	Histone H3.3
Q5E9F9	26S proteasome regulatory subunit 7
Q5E9H5	Mitochondrial chaperone BCS1
Q5E9H9	Palmitoyl-protein thioesterase ABHD10, mitochondrial
Q5E9I6	ADP-ribosylation factor 3
Q5E9K0	Proteasome subunit beta type-2
Q5E9Y9	Nucleoside diphosphate kinase 7
Q5EA79	Galactose mutarotase
Q5I597	Betaine--homocysteine S-methyltransferase 1
Q5W5H3	Neutrophil beta-defensin 3
Q5W5U3	hexokinase
Q5XQN5	Keratin, type II cytoskeletal 5
Q6B857	Cilia- and flagella-associated protein 20
Q6LBN7	Lactoferrin
Q6Q137	Septin-7
Q6QRN6	NADP H-hydrate epimerase
Q6QTG1	NADH-ubiquinone oxidoreductase chain 5
Q6QTH1	NADH-ubiquinone oxidoreductase chain 1
Q6R8F2	**Cadherin-1**
Q6VBM2	Phosphoribosylaminoimidazole carboxylase
Q6YFP9	Cytochrome c oxidase subunit 6B2
Q70IB2	Inactive ribonuclease-like protein 10
Q75WB5	5-oxoprolinase
Q76LV1	Heat shock protein HSP 90-beta
Q7YRQ8	Tissue factor pathway inhibitor 2
Q861T4	Similar to superoxide dismutase
Q862J3	V-type proton ATPase subunit D
Q865R1	Peroxisomal N
Q8HXG5	NADH dehydrogenase 1 beta subcomplex subunit 11, mitochondrial
Q8HXG6	NADH dehydrogenase 1 alpha subcomplex subunit 11
Q8HZY1	Serine protease inhibitor clade E member 2
Q8MJN0	FUN14 domain-containing protein 2
Q8SPP7	Peptidoglycan recognition protein 1
Q8SQ21	Adenosine 5'-monophosphoramidase HINT2
Q8WNR4	Histone H2B subacrosomal variant
Q95114	Lactadherin

Q95KV7	NADH dehydrogenase 1 alpha subcomplex subunit 13
Q95KW3	NADP arginine ADP-ribosyltransferase
Q95KZ6	Enoyl-CoA hydratase
Q95M18	Endoplasmin
Q9BE39	Myosin-7
Q9BGI1	Peroxiredoxin-5, mitochondrial
Q9BGU5	Cathepsin D
Q9GL30	Phospholipase B-like 1
Q9MZ13	Voltage-dependent anion-selective channel protein 3
Q9MZG3	Diazepam-binding inhibitor-like 5
Q9N285	Mitochondrial carrier homolog 2
Q9N2I2	Plasma serine protease inhibitor
Q9N2J2	Phospholipid hydroperoxide glutathione peroxidase
Q9TS96	Thymus HYPOCHOLESTEROLEMIC factor
Q9XS94	Major fibrous sheath protein
Q9XSC9	Transcobalamin-2
Q9XSG3	Isocitrate dehydrogenase [NADP] cytoplasmic
Q9XSJ4	Alpha-enolase
U3GR08	NADH-ubiquinone oxidoreductase chain 4
W0UV03	Ribonuclease A C1
W0UVF3	Ribonuclease A M1
X5F5B4	Serpin B4-like protein

Table S4. Differentially abundant proteins in sperm extract from Nellore bulls at rest and during sexual activity. The abundance of the proteins was estimated by peak area.

UniProt ID	Description	Differentially Expressed Proteins	
		First ejaculate proteins	Last ejaculate proteins
Q2KIC7	Serine/threonine-protein phosphatase	UP	
E1BKH1	EF-hand domain-containing protein 1	UP	
F1MUF4	Beta-galactosidase	UP	
Q2KIM0	Tissue alpha-L-fucosidase	UP	
Q2YDN8	Inactive serine/threonine-protein kinase VRK3	UP	
E1BCN4	AMP-binding domain-containing protein	UP	
A8E4P3	STOM protein		UP
Q6R8F2	Cadherin-1		UP
A0A3Q1MQK5	Midkine		UP
P22226	Cathelicidin-1		UP
P31976	Ezrin		UP
A5D9D1	Vanin 2		UP
B0JYN1	Cathepsin L2		UP
Q5DPW9	Cystatin E/M		UP
F1N430	Metalloproteinase inhibitor 2		UP

B0JYQ0	ALB protein	UP
A0A3Q8WRY0	S100 calcium binding protein A9	UP
A0A3Q1LXA8	inorganic diphosphatase	UP
A0A3Q1LS74	Complement factor H	UP
A0A3Q1MI01	Prosaposin	UP
P28782	Protein S100-A8	UP
P17697	Clusterin	UP
F1MLW2	BPI fold-containing family B member 1	UP
P81187	Complement factor B	UP
Q3ZC64	Ephrin-A1	UP
Q58DP6	Ribonuclease 4	UP
D4QBB3	Hemoglobin beta	UP
F1N650	Annexin	UP
F1MS23	Lipocln_cytosolic_FA-bd_dom domain-containing protein	UP
Q2UVX4	Complement C3	UP
P01966	Hemoglobin subunit alpha	UP
A5PJL8	C1QTNF5 protein	UP
P29392	Spermadhesin-1	UP
A0A3Q1MKC8	Keratin type II	UP
A6QP39	MSLN protein	UP
A0A452DHZ5	Nucleobindin-1	UP

5.1.References

1. Burns, B., Fordyce, G. & Holroyd, R. A review of factors that impact the capacity of beef cattle females to conceive, maintain a pregnancy, and wean a calf—Implications for reproductive efficiency in northern Australia. *Anim. Reprod. Sci.* **122**, 1-22 (2010).

2. Marshall, K. *et al.* Livestock Genomics for Developing Countries – African Examples in Practice. *Front. Genet.* **10**, 297 (2019).

3. Mwangi, F. *et al.* Diet and Genetics Influence Beef Cattle Performance and Meat Quality Characteristics. *Foods.* **12**, 648 (2019).

4. Gonzalez-Quintero, R. *et al.* Environmental impact of primary beef production chain in Colombia: Carbon footprint, non-renewable energy, and land use using Life Cycle Assessment. *Sci Total Environ.* **773**, 145573 (2021).

5. Mueller, M. & Van Eenennaam, A. Synergistic power of genomic selection, assisted reproductive technologies, and gene editing to drive genetic improvement of cattle. *CABI Agric Biosci.* **3**, 13 (2022).

6. Daly, J., Smith, H., McGrice, H, Kind, K. & Wettere, W. Towards Improving the Outcomes of Assisted Reproductive Technologies of Cattle and Sheep, with Particular Focus on Recipient Management. *Animals.* **2**, 293 (2020).

7. Miller, S. Genomic selection in beef cattle creates additional opportunities for embryo Technologies to meet industry needs. *Reprod. Fertil. Dev.* **35**, 98-105 (2023).

8. Baruselli, P., Ferreira, R., Sá, M. & Bó, G. Review: Using artificial insemination *v.* natural services in beef herds. *Animal.* **12**, 45-52 (2018).

9. Raidan, F. *et al.* Selection of performance-tested young bulls and indirect responses in commercial beef cattle herds on pasture and in feedlots. *Genet. Sel. Evol.* **48**, 85 (2016).

10. Capela, L., Leites, I., Romão, R., Lopes-da-Costa, L. & Pereira, R. Impact of heat stress on bovine sperm quality and competence. *Animals.* **12**, 975 (2022).

11. Klein, E. *et al.* The future of assessing bull fertility: Can the omics fields identify usable biomarkers? *Biol. Reprod.* **106**, 854-864 (2022).

12. Sweett, H. *et al.* Genome-wide association studies to identify genomic regions and positional candidate genes associated with male fertility in beef cattle. *Sci. Rep.* **10**, 20102 (2020).

13. Wells, M., Wondafrash, T., Awa, A. & Stephens, D. Effect of sexual rest and subsequent regular collection on acrosome characteristics of bull spermatozoa. *J. Anim. Sci.* **31**, 67-71 (1970).

14. Firman, R., Young, F., Rowe, D., Doung, H. & Gasparini, C. Sexual rest and pos-meiotic sperm aging in house mice. *J. Evol. Biol.* **28**, 1373-1382 (2015).

15. Barth, A. Sperm accumulation in the ampullae and cauda epididymides of bulls. *Anim. Reprod. Sci.***102**, 238-246 (2007).

16. Fernandez, B. *et al*. Cauda epididymis-specific beta-defensin 126 promotes sperm motility but not fertilizing ability in cattle. *Biol. Reprod.* **95**, 122 (2016).

17. Nixon, B. *et al.* Proteomic profiling of mouse epidymosomes reveals their contributions to post-testicular sperm maturation. *Mol. Cell Proteomics.* **18**, 91-108 (2019).

18. Hettyey, A., Vági, B., Penn, D., Hoy, H. & Wagner, R. Post-Meiotic Intra-Testicular Sperm Senescence in a Wild Vertebrate. *Plos One.* **7**, 50820 (2012).

19. Gasparini, C., Devigil, A. & Pilastro, A. Sexual selection, and aging: interplay between pre- and post-copulatory traits senescence in the guppy. *Proc. R. Soc. B.* **286,** 20182873 (2019).

20. Sepil, I. *et al.* Male reproductive aging arises via multifaceted mating-dependent sperm and seminal proteome declines but is postponable in *Drosophila*. *PNAS.* **117**,17094-17103 (2020).

21. Noguera, J., Dean, R., Isaksson, C., Velando, A. & Pizzari, T. Age-specific oxidative status and the expression of pre- and postcopulatory sexually selected traits in male red junglefowl, Gallus gallus. *Ecol. Evol***. 2**, 2155-2167 (2012).

22. Aitken J. Impact of oxidative stress on male and female germ cells: implications for fertility. *Reproduction.* **159**, 189-201 (2020).

23. Mancini, A., Oliva, A., Vergani, E., Festa, R. & Silvestrini, A. The dual of oxidants in male (in)fertility: Every rose has a thorn. *Int. J. Mol. Sci.* **24**, 4994 (2023).

24. Gasparini, C., Kelly, J. & Evans, J. Male sperm storage compromises sperm motility in guppies. *Biol. Lett.* **10**, 20140681 (2014).

25. Alahmar, A. Role of oxidative stress in male infertility: An updated review. *J. Hum. Reprod. Sci.* **12**, 4-18 (2019).

26. Singhal, S. *et al.* Antioxidant role of glutathione s-transferases: 4-hydroxynonenal, a key molecule in stress-mediated signaling. *Toxicol. Appl. Pharmacol.* **289**, 361-370 (2015).

27. Asadi, A., Ghahremani, R. & Abdolmaleki, A. Role of sperm apoptosis and oxidative stress in male infertility: A narrative review. *Int. J. Reprod. Biomed*. **19**, 493-504 (2021).

28. Moazamian, R. *et al.* Oxidative stress and human spermatozoa: diagnostic and functional significance of aldehydes generated as a result of lipid peroxidation. *Mol. Hum. Reprod.***21**, 502-515 (2015).

29. Hamilton, T. *et al.* Induced lipid peroxidation in ram sperm: semen profile, DNA fragmentation, and antioxidant status. *Reproduction.* **151**, 379-390 (2016).

30. Mannucci, A. *et al.* The impact of oxidative stress in male infertility. *Front. Mol. Biosci.* **8**, 799294 (2022).

31. Phaniendra, A., Jestadi, D. & Periyasamy, L. Free radicals: properties, sources. targets and their implication in various diseases. *Ind. J. Clin. Biochem.* **30**, 11-26 (2015).

32. Yoshida, Y., Umeno, A., Akazawa, Y., Shichiri, M., Murotomi, K. & Horie, M. Chemistry of lipid peroxidation products and their use as biomarkers in early detection of diseases. *J. Oleo Sci*. **64**, 347–356 (2015).

33. Agarwal, A., Virk, G., Ong, C. & Plessis, S. Effect of oxidative stress on male reproduction. *J. Mens Health.* **32**, 1-17 (2014).

34. Collodel, G., Moretti, E., Noto, D., Corsaro, R. & Signorini, C. Oxidation of polyunsaturated fatty acids as a promising area of research in infertility. *Antioxidants.* **11**, 1002, 2022.

35. Collodel, G., Moretti, E., Noto, D., Lacoponi, F. & Signorini, C. Fatty acid profi, le, and metabolism are related to human sperm parameters and are relevant in idiopathic infertility and varicocele. *Mediators Inflamm.* **2020**, 3640450 (2020).

36. Zerbinati, C. *et al.* Fatty acids profiling reveals potential candidate markers of semen quality. *Andrology.* **4**, 1094-1101 (2016).

37. Collodel, G., Castellini, C., Lee, J. & Signorini, C. Relevance of fatty acids to sperm maturation and quality. *Oxid. Med. Cell. Longev.* **2020**, 7038124 (2020).

38. Kogan, T. *et al.* Association between fatty acid composition, cryotolerance, and fertility competence of progressively motile bovine spermatozoa. *Animals.***11**, 2948 (2021).

39. Esmaeili, V., Shahverdi, A., Moghadasian, M. & Alizadeh, A. Dietary fatty acids affect semen quality: a review. *Andrology,* **3**, 450-461 (2015).

40. Aiken, R., Wingate, J., De luliis, G., Koppers, A. & Mclaughlin, E. *Cis* –unsaturated fatty acids stimulate reactive oxygen species generation and lipid peroxidation in human spermatozoa. *J. Clin. Endocrinol. Metab.* **91**, 4145-4163 (2006).

41. Oddi, S. *et al.* Cryotolerance of equine spermatozoa correlates with the specific fatty acid pattern: A pilot study. *Theriogenology.* **172**, 88-94 (2021).

42. Prasinou, P. *et al.* The lipidomics of spermatozoa and red blood cells membrane profile of martina franca donkey: preliminary evaluation. *Animals.* **13**, 8 (2023).

43. Zhu, Z. Exogenous oleic acid and palmitic acid improve boar sperm motility via enhancing mitochondrial β-oxidation for ATP generation. *Animals.* **10**, 591 (2020).

44. Islam, M., Umehara, T., Tsujita, N. & Shimada, M. Saturated fatty acids accelerate linear motility through mitochondrial ATP production in bull sperm. *Reprod. Med. Biol.* **20**, 289-298 (2021).

45. Zhu, Z. *et al.* Gene expression and protein synthesis in mitochondria enhances the duration of high-speed linear motility in boar sperm. *Front Physiol.* **10**, 252 (2019).

46. Niki, E. Biomarkers of Lipid Peroxidation in Clinical Material. *Biochim. Biophys. Acta (Bba) - Gen. Subjects.* **1840**, 809–817 (2014).

47. Ikeda, S. & Yamada, M. Midkine and cytoplasmic maturation of mammalian oocytes in the context of ovarian follicle physiology. *Br. J. Pharmacol.* **171**, 827-836 (2013)

48. Massa, E., Prez, G., Zumoffen, C., Morente, C. & Ghersevich, S. S100 A9 is expressed and secreted by the oviduct epithelium, interacts with gametes and affects parameters of human sperm capacitation in vitro. *J. Cell. Biochem.* **120**, 17662-17676 (2019).

49. Gomes, F. et al. Protein signatures of seminal plasma from bulls with contrasting frozen-thawed sperm viability. *Sci. Rep*. **10**, 14661 (2020).

50. Rêgo, J. et al. Seminal plasma proteome of eletroejaculated Bos inducus bull. *Anim. Reprod. Sci*. **148**, 1-17 (2014).

51. Torabi, F., Bogle, O., Estanyol, J., Oliva, R. & Miller, D. Zona pellucida-binding protein 2 (ZPBP2) and several proteins containing BX7B motifs in human sperm may have hyaluronic acid binding or recognition properties. *Mol. Hum. Reprod.* **23**, (803-816) 2017.

52. Muramatsu, H. *et al.* Female infertility in mice deficient in midkine and pleiotrophin, which form a distinct family of growth factors. *Genes Cells.* **11**, 1405-1417 (2006).

53. O´Connor, B., Pope, B., Peters, M., Ris-Stalpers, C. & Parker, K. The role of extracellular matrix in normal and pathological pregnancy: Future applications of microphysiological systems in reproductive medicine. *Exp. Biol. Med.* **245**, 1163-1174 (2020).

54. Codognoto, V. et al. Functional insights into the role of seminal plasma proteins on sperm motility of buffalo. *Anim. Reprod. Sci.* **195**, 251-258 (2018).

55. Bezerra, M. et al. Major seminal plasma proteome of rabbits and associations with sperm quality. *Theriogenology*.**128**, 156-166 (2019).

56. Sayasith, K., Sirois, J. & Lussier, J. Expression, regulation, and promoter activation of vanin-2 (vnn2) in bovine follicles prior to ovulation. *Biol. Reprod.* **89**, 1-11 (2013).

57. Huang, S. *et al.* Maternal supply of cysteamine alleviates oxidative stress and enhances angiogenesis in porcine placenta. *J. Animal. Sci. Biotechnol.* **12**,91 (2021).

58. Perez-Patino. C. *et al.* The proteome of pig spermatozoa is remodeled during ejaculation. *Mol. Cell. Proteom. MCP.* **18**, 41-50 (2019).

59. Druart, X., Rickard, J., Tsikis, G. & de Graaf, S. Seminal plasma proteins as markers of sperm fertility. *Theriogenology.* **137**, 30-35 (2019).

60. Xu, F., Gou, G., Zhu. W. & Fan, L. Human sperm acrosome function assays are predictive of fertilization rate in vitro: a retrospective cohort study and meta-analysis. *Reprod. Biol. Endrocrinol.* **16**, 81 (2018).

61. Breitbart, H. & Shabtay, O. Sperm acrosome reaction. In: *Encyclopedia of reproduction, 2nd edition.* (ed. Skinner, M) 284-288 (Academic Press, 2018).

62. Kon, S. *et al.* Sperm storage influences the potential for spontaneous acrosome reaction of the sperm in the newt Cynops pyrrhogaster. *Mol. Hum. Reprod.* **84**, 1314-1322 (2017).

63. Aldana, A., Carneiro, J., Martinez-Mekler, G. & Darszon, A. Discrete dynamic model of the mammalian sperm acrosome reaction: the influence of acrosomal ph and physiological heterogeneity. *Front. Physiol.* **12**, 682790 (2021).

64. Huta, Y., Nitzan, Y. & Breitbart, H. Ezrin protects bovine spermatozoa from spontaneous acrosome reaction. *Theriogenology.* **151**, 119-127 (2020).

65. Rotfeld, H., Hillman, P., Ickowicz, D. & Breitbart, H. PKA and CaMKII mediate PI3K activation in bovine sperm by inhibition of the PKC/PP1 cascade. *Reproduction.* **147**, 347-356 (2014).

66. Phopin, K. *et al.* Roles of mouse sperm-associated alpha-L-fucosidases in fertilization. *Mol. Reprod. Dev.* **80**, 273-285 (2013).

67. Katano, M. et al. The juvenile myoclonic epilepsy-related protein EFHC1 interacts with the redox-sensitive TRPM2 channel linked to cell death. *Cell Calcium,* **51**, 179-158 (2012).

68. Hara, Y. et al. LTRPC2 Ca2+-permeable channel activated by changes in redox status confers susceptibility to cell death. *Molecular Cell.* **9**, 163-173 (2002).

69. Colégio Brasileiro de Reprodução Anima. Manual para exame andrológico e avaliação de sêmen animal. 3rd ed. Belo Horizonte, Brasil, 2013. pp. 15-30.

70. Siqueira, J. *et al.* Heritability estimate and genetic correlations of reproductive features in Nellore bulls, offspring of super precocious, precocious and normal cows under extensive farming conditions. *Reprod. Domest. Anim.* **47**, 313-318 (2012)

71. Blom, E. The ultrastructure of some characteristic sperm defects and a proposal for a new classification of the bull spermiogram. *Nord. Vet. Med.* **53**, 383– 391 (1973).

72. Bradford, M. A rapid and sensitive method for the quantitation of microgram quantities of protein utilizing the principle of protein-dye binding. *Anal. Biochem.* **72**, 248-254 (1976).

73. Dieterich, S., Bieligk, U., Beulich, K., Hasenfuss, G.& Prestle, J. Gene expression of antioxidative enzymes in the human heart: increased expression of catalase in the end-stage failing heart. *Circulation.* **101**, 33-39 (2000).

74. Aebi, H. Catalase in vitro. In: *Methods in Enzymology*. 121–126 (Elsevier, 1984).

75. Habig, W., Pabst, M. & Jakoby, W. Glutathione S-transferases. The first enzymatic step in mercapturic acid formation. *J. Biol. Chem.* **249**, 7130–7139 (1974).

76. Tsikas, D. Analysis of nitrite and nitrate in biological fluids by assays based on the Griess reaction: Appraisal of the Griess reaction in the l-arginine/nitric oxide area of research. *J Chromatogr B analyt Tecnhol Biomed Life Sci.* **851**, 51–70 (2007).

77. Buege, J. & Aust, S. Microsomal lipid peroxidation. In: *Methods in Enzymology* (ed. Fleischer, S. & Packer, L), 302–310 (Academic Press, 1978).

78. Corradini, G. *et al*. Plasma fatty acid lipidome is associated with cirrhosis prognosis and graft damage in liver transplantation. *Am J Clin Nutr* **100**, 600–608 (2014).

79. Laemmli, K. Cleavage of structural proteins during the assembly of the head of bacteriophage T4. *Nature.* **227**, 680-685 (1970).

80. Resjö, S. *et al.* Proteomic analysis of Phytophthora infestans reveals the importance of cell wall proteins in pathogenicity. *Mol. Cell. Proteomics.* **16**, 1958-1971 (2017).

81. Shevchenko, A., Tomas, H., Havlis, J., Olsen, J. & Mann, M. In-gel digestion for mass spectrometric characterization of proteins and proteomes. *Nat. Protoc.* **1**, 2856-2860 (2006).

82. Ma, B. et al. PEAKS: powerful software for peptide *de novo* sequencing by tandem mass spectrometry. *Rapid Commun. Mass Spectrom.* **17**, 2337-2342 (2003).

83. Altschul, S., Gish, W., Miller, W., Myers, E. & Lipman, D. Basic local alignment search tool. *J. Mol. Biol.* **215**, 403-410 (1990).

84. McDonagh, B., Sakellariou, G., Smith, N., Brownridge, P. & Jackson, M. Differential cysteine labeling and global label-free proteomics reveals an altered metabolic state in skeletal muscle aging. *J. Proteome Res.* **13**, 5008-5021 (2014).

85. Tatusov, R. *et al.* The COG database: an updated version includes eukaryotes. *BMC Bioinformatics.* **4**, 41 (2003).

86. Kanehisa, M., Sato, Y. & Morishima, K. BlastKOALA and GhostKOALA: KEGG tools for functional characterization of genome and metagenome sequences. *J. Mol. Biol.* **428**, 726-731 (2016).

6. FINALS CONSIDERATIONS

- Sexual rest is a transient, reversible condition that leads to the accumulation of spermatozoa in the tail of the epididymis. The sperm characteristics resulting from prolonged accumulation are incompatible with the fertility of bulls.

- Andrological examination is the best way to diagnose and reverse sexual rest.

- The sperm characteristics exhibited by bulls at sexual rest are a product of the oxidative imbalance of the epididymal environment.

- Excessive production of reactive oxygen species causes morphological changes in spermatozoa, accelerates sperm capacitation and acrosomal reaction and causes the death of sperm cells.

- The results of the present work constitute a source of basic knowledge that can help clarify the molecular events of sexual rest in spermatozoa.

- Future studies should address the causes that lead to the accumulation of sperm in extragonadal reserves.